A model of neuron-glia crosstalk explains stages of neural tissue resilience

Andreas Nold *[1], Danylo Batulin[1], Katharina Birkner[2], Stefan Bittner †[2], and Tatjana Tchumatchenko †‡[1]

[1]Theory of Neural Dynamics, Max Planck Institute for Brain Research, Frankfurt, Germany
[2]Department of Neurology, Focus Program Translational Neuroscience (FTN), University Medical Center of the Johannes Gutenberg University Mainz, Mainz, Germany

November 1, 2019

Abstract

The human brain keeps billions of neurons functional across decades. Glia, the helper cells of the brain, are essential to maintaining this neural resilience: They react to neuronal states and carefully balance either quick repair or disposal of injured neurons to prevent damage spread. Malfunction of these interactions is implicated in many neurodegenerative diseases. Here, we propose a model for neuron-glia crosstalk which maintains tissue resilience by a balance between housekeeping and damage-inducing glial reactions to neuronal damage and death. Depending on the interplay of the functionality of this crosstalk, the model assumes four distinct tissue states: healthy, challenged, primed tissue at risk of acute damage propagation, and chronic neurodegeneration. These states and their underlying mechanisms are in agreement with experimental observations for the most common neurodegenerative conditions. We suggest that the onset of neurodegeneration results from a compromise between two conflicting goals: Maintenance of short-term resilience to stressors, and resilience to degeneration. Based on these findings, we discuss disease-state specific diagnostic and therapeutic strategies.

1 Introduction

The human brain faces the challenge of keeping neuronal networks functional throughout many decades. This requires repairing injured neurons or, if their damage is irreversible, disposing of them. The decision of what to do with injured neurons is made by interactions between glia, the helper-cells of the brain, and neurons [15, 3, 5], and needs to be carefully balanced: neuronal disposal has to be kept low, as neurons only have a limited potential for regeneration [5]. On the other hand, if disposal processes are dysfunctional, then damage spreads to neighbors and synaptic partners [58]. Thus, the regulation of repair-or-dispose decisions is essential for the maintenance of global tissue health, tissue resilience and prevention of neurodegenerative

*andreas.nold@brain.mpg.de; Corresponding author
†Contributed equally.
‡tatjana.tchumatchenko@brain.mpg.de; Corresponding author

diseases [52, 54, 51]. Are inaccurate repair-or-dispose decisions to blame for the loss of resilience? We set up a computational model which combines short-term neuronal disposal decisions with slow damage-accumulation and neurodegenerative processes. We show that these two effects define four distinct tissue states which correspond to phases in common neurodegenerative conditions. We argue that neurodegeneration ensues when maintenance of short-term stability and long-term resilience become conflicting goals.

Glial cells have long been regarded as secondary 'helper cells' of the brain. Microglia surveil their local microenvironment, clear the tissue of pathogens and phagocyte debris [80]; and astrocytes provide trophic support and housekeeping functions [61]. However, recent genetic and experimental results have shed light on a more diverse and complex set of glial functions [84, 61, 65], which include highly reactive and pro-inflammatory phenotypes that can inflict neural damage [67]. Intriguingly, in the healthy brain, both damage-repairing and damage-inducing glial activity can have a net homeostatic function in maintaining resilience, by either repairing or removing stressed neurons.

Recent experimental work has shown that these originally homeostatic glial processes can become dysfunctional and harm tissue resilience [52, 54, 51]. The causes of a malfunction can be complex and multi facetted, ranging from cardiovascular stress [88] to meningeal lymphatic dysfunction [23] and a dysfunctional immune communication across the gut-brain axis [103]. Ultimately, they can result in neurodegeneration and functional deficits. But even in neurodegeneration, glia can have a dual role – their reactive phenotype activation can be detrimental in one condition while serving a neuroprotective role in another [87]. For instance, accumulation of senescent microglia and astrocytes can drive tau aggregation and cognition-associated neuronal loss [17], or microglia can contribute to protein clearance [52] and promote recovery from motor symptoms in an amyotrophic lateral sclerosis model [98]. Functional glia-neuron feedback is therefore critical for resilience against neurodegeneration, containment of lesions, and maintenance of neuronal network function [42, 16].

The case-dependent, dual role of glial activation for neuronal health emphasizes the need to complement experimental one-interaction-at-a-time approaches by a study of systems-level phenomena. In this work, we build on the successes of reductionist approaches in biology [7, 6] and neuroscience [1, 2] and propose a computational model which incorporates damage-repairing versus damage-inducing glial activity at a neuronal population level. This reveals long- and short term implications of individual repair-or-dispose decisions.

Specifically, we show how the interplay between long-term stressors and the adaptation of (1) glial reactivity, (2) spatial focal range and (3) glial reaction to cell death lead to four distinct tissue states: Healthy tissue with intact seed removal; challenged tissue with decreased functionality and accuracy of glia-neuron crosstalk, primed tissue which is functional, but can become unstable and fuel quickly spreading lesions in the event of a large enough external shock; and finally chronic degeneration, in which seed removal breaks down, giving way to neurodegenerative processes. We show under which conditions a neuronal population can become either vulnerable to acute damage spread or promote slow neurodegeneration, and link these distinct tissue states to the most common neurodegenerative conditions and their phases.

The structure of the paper is as follows: We introduce key features of the model in Sec. II-A, and discuss the model equations of slow and fast processes in sections II-B and II-C, respectively. In sections II-D and II-E, we discuss implications of two aspects of fast neuron-glia crosstalk. In section II-F and II-G, we discuss the four distinct tissue states that we identify based on our analysis. In section III, we discuss links between the tissue states and progression of Alzheimer's (III-A), and Multiple sclerosis (III-B). Common risk factors such as aging, and possible implications of our model for therapy, are discussed in III-C and III-D.

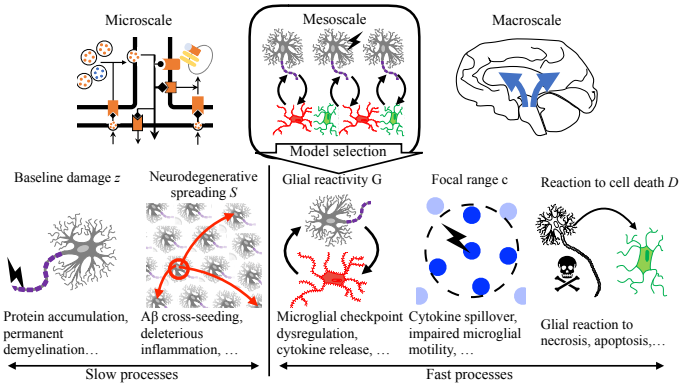

Figure 1: **Five classes of neuron-glia crosstalk are included in a mesoscale model.** We choose a mesoscopic modeling level which generalizes tissue response to a small number of observable factors. It mediates between the microscopic level of cellular and molecular processes [56] (top left) and the macroscopic level of interacting brain regions [57, 108] (top right). We include five distinct properties of neuron-glia crosstalk (see Eqs. 1, 2): (i) accumulation of non-repairable baseline damage (z); (ii) slow neuron-to-neuron spreading of baseline damage (S); (iii) glial reactivity to neuronal damage (G); (iv) focal range of glial reactivity (c); (v) tissue reaction to cell death (D).

2 Results

2.1 Key features of neuron-glia crosstalk

We aim to capture basic principles of tissue behavior with a minimal number of parameters (see Fig. 1). Our model therefore operates at the mesoscopic level and mediates between microscopic descriptions of individual signaling pathways [29] and the macroscopic descriptions of different brain regions [57, 108]. This allows us to group key processes of neuron-glia crosstalk into five classes operating on two timescales (see also Appendix, Fig. 6).

The first two classes represent slow, neurodegenerative processes: (i) Accumulation of non-repairable baseline damage such as misfolded protein accumulation [41] or permanent demyelination [72] are represented by the variable z; (ii) Slow increase and spread of this damage is represented by the dimensionless parameter S. S is a measure for how many neurons will be affected by the baseline damage of one neuron (see Eq. 5). Processes represented by this class include intracellular 'protein condensation' [93, 40], self-propagating protein assemblies [102, 58] and the vicious cycle of deleterious inflammation and neurodegeneration [10, 111].

The other three classes describe fast processes of neuron-glia crosstalk: (iii) The amount of glial reactivity to neuronal damage is captured by the variable G. It describes the ability to activate damage-inducing effects on neurons such as the glial release of pro-inflammatory cytokines and microglial checkpoint dysregulation [54]; (iv) Spatial effects such as impairment of microglial motility [24] and cytokine spillover are represented by the focal range parameter c. The narrow and wide limiting cases $c \to 0$ and $c \to 1$ represent glia reacting independently to each neuron, or collectively to all neurons, respectively; (v) Tissue reactions to the death of a neuron are captured by the parameter D. Once a neuron dies, necrosis or apoptosis results in either damage-inducing or damage-repairing effects on neighboring neurons [4]. This is captured by positive and negative values for D, respectively (see Appendix, Sec. A for further detail).

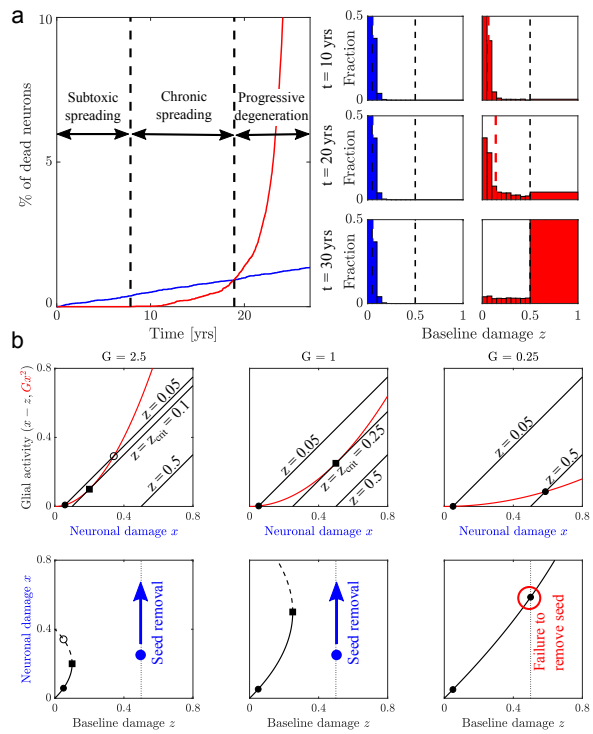

Figure 2: **Active removal of seed neurons maintains long-term resilience. a**, Tissue behavior with and without active seed-removal at $z = 0.5$, depicted by blue and red lines, respectively. In both tissues seeds of degeneration are generated at a constant rate ν. Failure to remove seeds leads to slow neurodegeneration progression in three phases, but seed removal maintains long-term resilience. **b**, A balance between damage-repairing housekeeping effects (black lines) and damage-inducing effects (red lines) implements active seed-removal. High reactivity G ensures early seed removal, and low reactivity G leads to failure of seed removal.

2.2 Active seed removal prevents spreading of slow neurodegeneration

Slow neuron-to-neuron spread of damage is modeled as follows: Each neuron n is assigned a dimensionless value z_n describing its non-repairable baseline damage. $z_n = 0$ denotes baseline health and $z_n = 1$ represents an amount of damage which induces cell-death. $z_{\text{cliff}} = 0.5$ defines a seeding threshold which acts similar to a catastrophic cliff e.g. in protein aggregation [40]. Neurons whose damage exceeds z_{cliff} serve as seeds. A seeding neuron n propagates damage to other neurons, and every neuron is linked to M potential seeds, defined by the set $\mathcal{C}_n$. In the following, we refer to a neuron whose damage is $z_n \geq z_{\text{cliff}}$ as a 'seed'. To mimic random damage-inducing events at times $t_{k,n}$ due to age, stress or neuronal susceptibility [40], we include a slow background seeding rate ν. The model equations take the form

$$\frac{\mathrm{d}z_n}{\mathrm{d}t} = \frac{1}{\tau_\infty} \sum_{m \in \mathcal{C}_n} [z_m - z_{\text{cliff}}]_+ + z_{\text{cliff}} \sum_k \delta\left(t - t_{k,n}\right), \tag{1}$$

where $[z]_+ = z$ for $z > 0$ and zero otherwise. τ_∞ is the characteristic time scale for slow stress-accumulating processes and is here in the timescale of decades. In the early phase of damage propagation, before neurons

die, the damage susceptibility of a network is determined by the dimensionless parameter $S = M/(\nu\tau_\infty)$. It represents the ratio between the rate of damage propagation, given by the number M of neighbors damage is spread to per time unit τ_∞, and the frequency ν of random seed-generating damage events (see Appendix, Eq. 5).

Neurodegenerative spread modeled in Eq. 1 progresses in three phases (see Fig. 2a). First, damage spreads subtoxically: seeds are formed and damage spreads, but does not yet induce cell death. In a second chronic spreading phase, the number of seeds increases and damage spread accelerates. However, death rates are still low. The final phase is characterized by widespread damage and exponential cell loss. This breakdown of long-term resilience can be avoided if neurons are selectively removed. An effective selection mechanism maintains neurons if their baseline damage is low ($z_n < z_{\text{cliff}}$), but actively removes them as soon as the baseline damage crosses the seeding threshold z_{cliff}. The rate of neuronal deaths then reaches its lowest possible value corresponding to the background seeding rate ν (see Fig. 2a).

2.3 Balance of housekeeping and damage-inducing neuron-glia crosstalk allows for active seed-removal

An active seed-removal mechanism repairs neurons if damage is low, but disposes of them if damage exceeds the seeding threshold z_{cliff}. The simplest formalization of such a mechanism is through neuron-glia feedback which tips in favor of damage-inducing effects once the baseline damage z_n of a neuron crosses a threshold (see Appendix, Sec. A.2 for a discussion of possible biological mechanisms). This threshold needs to be lower than the seeding threshold z_{cliff}. To formalize this, we introduce x_n as acute neuronal damage which assumes values between zero and unity, whereby 0 represents health and 1 denotes cell death. x_n is dynamically modulated by a balance of damage-inducing and damage-repairing mechanisms. Here, the baseline damage z_n inhibits repair functions. For simplicity, we assume that the neurons are organized in a periodic equidistant one- or two dimensional grid at positions $\mathbf{r}_n$ with grid spacing of one. We also assume that damage-inducing effects g_n scale quadratically with acute damage x_n and are controlled via the glial reactivity parameter G:

$$\tau\frac{\mathrm{d}x_n}{\mathrm{d}t} = -\underbrace{(x_n - z_n)}_{\text{repair}} + \underbrace{\frac{1-c}{1+c}\sum_m c^{|\mathbf{r}_n-\mathbf{r}_m|} g_m}_{\text{damage-inducing effects}} \tag{2a}$$

$$\text{with} \qquad g_n = \begin{cases} Gx_n^2 & \text{if } n \in \mathcal{S}_{\text{alive}}(t) \\ De^{-\frac{t-t_n^{\text{death}}}{\tau_{\text{death}}}} & \text{else} \end{cases}, \tag{2b}$$

where for simplicity $\tau = 4\text{h}$ is set to the timescale of the microglial screening cycle [80]. The spatial impact of one neuron to another is represented by the sum in Eq. 2a. $c \in [0, 1]$ is the focal range of glial reactivity, with $c \to 0$ being a perfectly focused reactivity. Once a neuron dies at time t_n^{death}, it elicits an anti- (for $D < 0$) or pro-inflammatory (for $D > 0$) glial reaction which decays exponentially with time constant $\tau_{\text{death}} = 24\text{h}$ (see Eq. 2b). $\mathcal{S}_{\text{alive}}(t) = \{n : x_n(t') < 1 (\forall t' \leq t)\}$ is the set of indices of all alive neurons at time t.

First, consider a system with narrow focal range (small c). Steady states of the tissue are obtained by balancing damage-inducing effects Gx^2 and damage-repairing effects $x - z$ for each neuron (see Eq. 2a). If the effective parameter

$$H = 4Gz \tag{3}$$

is less than unity, $H < 1$, the system has one stable and one unstable steady state (see Fig. 2b). Once H crosses unity, the neuron is driven to cell death. By tuning glial reactivity G, the tissue sets the threshold $z_{\text{crit}} = 1/4G$, beyond which a neuron is actively removed. For a more details, see Appendix, and Appendix,

Sec. B. This process results in a controlled seed-removal mechanism – therefore preventing slow damage-spreading and maintaining long-term tissue resilience.

2.4 Increasing focal range of neuron-glia crosstalk compromises seed removal

An increase of the glial focal range c, e.g. due to dysfunctional or impaired glial motility [24], has dramatic effects for seed removal. It means that the threshold damage level $z_{\text{crit}}^{\text{single}}$ beyond which a single neuron is removed can be much greater than the system-level threshold z_{crit} (see Fig. 3 and Appendix Fig. 7). For systems with a narrow focal range $c \to 0$, $z_{\text{crit}}^{\text{single}}$ is equal to z_{crit}. But, for systems with a wide focal range $z_{\text{crit}}^{\text{single}}$ can be significantly higher. This means that seeds might not be removed, or that removal is slower and puts more stress on the surrounding tissue (see Fig. 3).

Whether seed removal is functional or not depends on the interplay between the focal range c and two other factors: First, average non-repairable baseline damage z across the neuronal population needs to be low, such that highly damaged neurons can be singled out. Second, glial reactivity to neuronal damage G needs to be high to initiate removal. If, however, reactivity G is too high, the system becomes unstable. Reconciling seed-removal and stability of the population increasingly restricts the parameter space as the mean baseline damage $\langle z \rangle$ increases (See Appendix, Fig. 8). Maintenance of short- and long-term resilience therefore become conflicting goals in age and disease.

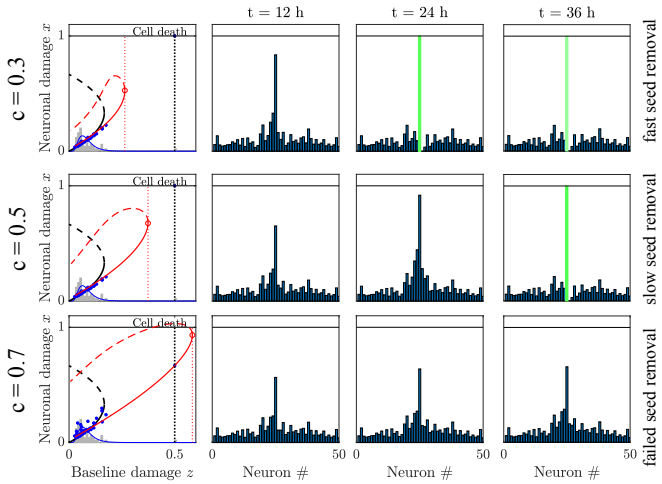

Figure 3: **Wide focal range critically slows down seed removal or leads to failure of seed removal.** Figures depict the reaction of a healthy population of neurons with $\langle z \rangle = 0.05$ to baseline damage induction of one neuron. Left column: Black solid and dashed line as in Fig. 2. The red line is the stability line for a single neuron in the population. Each blue dot represents one neuron of the population, grey bars represent the histogram of the baseline damage. Right bar graphs: Reaction of the neuron population over time if z_{25} is set to 0.5 at $t = 0$. Narrow focal range leads to swift recognition and removal of a seed. Wider focal ranges delay seed removal and affects a larger part of neighboring tissue ($c = 0.5$). $c = 0.7$ leads to failure of seed removal and permanently affects surrounding tissue. (see Appendix Fig.8 for details).

2.5 Tissue reaction to cell death defines short term resilience

If baseline damage z becomes too large, then short-term damage-inducing glial activity can compromise short-term tissue stability (see Fig. 4a). This can happen in two ways: First, a sudden large increase of $\langle z \rangle$ can lead to spontaneous cell death across the tissue. This has different consequences, depending on the focal range c (see Appendix, Fig. 9): Systems with narrow focal ranges react gradually to an increase of $\langle z \rangle$, but systems with wide focal range c react suddenly and collectively. This population effect has been observed in many other biological and ecological systems, for instance when coral reefs are repaired by 'mobile link organisms' from nearby reefs [91].

In addition to this classical transition, our model also reveals a 'primed state' for intermediate increases of $\langle z \rangle$. Under normal conditions, this primed tissue appears to be healthy, but in the event of strong enough acute stress, it amplifies damage and may initiate a wave-like spreading lesion. In general, protective glial reactions to neuronal cell death (low D) protect the surrounding tissue against these knock-on effects. If this protection, however, is attenuated, and glial focal range is wide, then acute attacks can cause widespread damage. Glial reactivity with wide focal range (high c) and pro-inflammatory glial reaction to cell death (high D) increases damage. The danger of acute short-term damage amplification is more pronounced for a system with intact, high, glial reactivity G (see Appendix, Fig. 10 for details).

2.6 Tissue states

Our parameter study reveals four states which characterize neural tissue resilience: healthy tissue, challenged tissue, tissue prone to acute lesion spread, and chronically inflamed tissue (see Table 1). In healthy tissue, microglia surveil the tissue and respond focally to the state of single neurons – by either repairing or removing the compromised seed. In this state, which is characterized by low baseline damage z, high reactivity G, a narrow focal range (low c), and a protective tissue reaction to cell death (low D), short- and long-term resilience are maintained.

In age or disease, baseline neuronal damage z accumulates and microglial function becomes increasingly dysregulated [105]. In our model, this challenged tissue exhibits increased values of z and c and requires a down-regulation of tissue reactivity G in order to maintain short-term stability. Notably, active seed removal is still functional in this state. It is, however, slowed down and perturbations of the tissue are resolved at a slower pace (see Fig. 3). This phase is crucial for disease progression. Once the reserve of this phase is exhausted and seed removal fails, slow, disease-specific mechanisms take over, and the tissue transitions to the chronic phase.

If reactivity G is not down-regulated with increasing baseline damage z, then neural tissues enters a primed state. In this state, the tissue appears to be healthy, but in the event of a sufficiently strong acute attack, glial reactivity exacerbates the effect of the attack, and can lead to a quickly spreading lesion (Fig. 4). In the event of a large shift in conditions, the whole system may become unstable, leading to spontaneous cell death across the tissue. The primed state can be aggravated and triggered more easily if glial reaction to cell death does not protect surrounding neurons, therefore allowing for a fast domino-like passing on of neurodegeneration to neighboring tissue (see Appendix, Fig. 10).

The chronic, and for most neurodegenerative diseases final, phase is characterized by a widening of focal range c and loss of reactivity G, leading to a failure of active seed removal, and therefore a breakdown of long-term resilience. While glial reactivity G is down-regulated, glial activity Gx^2 is high due to high levels of baseline damage z and consequently high levels of acute damage x. This reflects chronically inflamed conditions in neurodegenerative diseases which are ineffective in resolving inflammation. Interestingly, in this state the down-regulated glial reactivity protects the tissue against unwanted amplification of acute attacks (see Fig. 4c), and may therefore also be a self-protective measure.

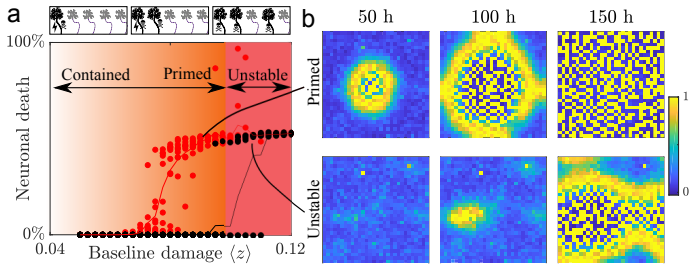

Figure 4: **Primed tissue is susceptible to damage amplification of acute attacks.** Simulation of a population of neurons with high reactivity $G = 2$, widened focal range $c = 0.4$, and inhibited resolution of activity after cell death $D = -0.5$. Left: High population-wide damage levels $\langle z \rangle$ can destabilize the tissue and lead to spontaneous cell death (black line). In primed, but otherwise stable tissue, an acute attack can initiate an expanding lesion (red line). Each dot represents one simulation. Right: Acute damage levels x. Top right: Snapshots for a spreading damage reaction following an acute attack for a primed tissue with mean damage $\langle z \rangle = 0.085$. Bottom right: Snapshots for a tissue reaction to a population-wide increase of baseline damage to an unstable regime $\langle z \rangle = 0.11$.

2.7 The transition from the challenged to the chronic phase

We subject two model systems to repeated low subthreshold stressors (see Fig. 5). In the first scenario, the stressors are more frequent, weaker, and more distributed across the tissue. In the second scenario the stressors are less frequent, stronger, and are focused in one position. The longer the system takes to resolve the stressor, the more does the baseline damage z_n increase. Glial reactivity G and focal range adapt to the increasing spatially heterogeneous baseline damage such that short term stability is maintained (see Appendix, Fig.11 for how a lack adaptation of G and c leads to early catastrophic neuron loss).

In the first, distributed stress example, glial reactivity G steadily declines, until seed removal breaks down. Once seeds are not removed, the focal range c increases to maintain system stability. In the next phase, damage accumulation accelerates, but damage remains below the neuronal deaths threshold. In the final phase, massive neuron death is observed. The situation is slightly different for a focal, less frequent stressor. In this scenario, the baseline damage only increases in a very narrow domain, and therefore mean baseline damage levels are very low. Strikingly, however, the 'footprint', or net impact of each stress event, increases dramatically as the transition point to the chronic phase is approached. After seed removal breaks down, a decrease in glial reactivity G and increase in focal range c reduces the impact of the external stressors, and instead slow neurodegenerative processes take over to drive baseline damage accumulation.

3 Discussion

Glia play an important role in neuronal tissue maintenance. Not only do they provide trophic support and repair damage, but they can also induce damage. Mechanistically, these processes of neuron-glia crosstalk are well-documented (see Appendix, Sec. A for a detailed discussion). We propose a model for the active removal of seeds, based on the interplay of these mechanisms. What role do these repair-or-dispose decision have for long-term tissue resilience and neurological disease progression? Intriguingly, the challenged, primed and chronic phases, which we found in our model, share common features and key processes with Alzheimer's disease, a classical neurodegenerative condition, multiple sclerosis, a neuroinflammatory disorder, and with other neurological diseases. Therefore, even though evidence suggests that overlap of genetic susceptibility

	(i) Healthy	(ii) Challenged	(iii) Primed	(iv) Chronic
Tissue properties	Tightly regulated tissue surveillance	Damage accumulation, lowered microglial motility	Up-regulated phagocytosis, primed microglia	Dysregulated innate immune response, chronic neuronal stress
Parameters Baseline damage z Glial reactivity G Glial focal range c Reac. to cell death D	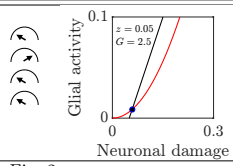	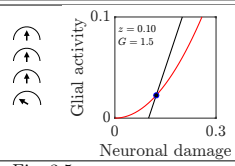	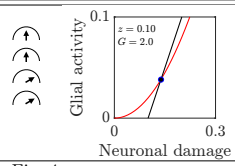	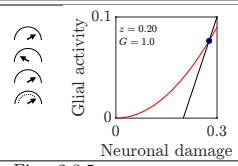
Prediction	Fig. 2	Fig. 3,5	Fig. 4	Figs. 2,3,5
Seed removal	✓	weakened	weakened	×
Contains acute attack	✓	weakened	×	∼
Inflammation $\langle Gx^2 \rangle$	Focused and functional	Limited functionality	Damage-amplifying	High, dysfunctional
Clinical outcome	Maintenance of short- and long-term resilience	Subclinical disease activity, driven by the periphery (e.g. RRMS)	Immune training, acute lesion propagation	Neurodegeneration, chronic inflammation (e.g. SPMS)
Therapy	-	Control G, keep c low.	Adapt G, lower c, D.	Reduce G.

Table 1: **Four characteristic states of neuron-glia crosstalk and their impact on tissue resilience** (i) In the healthy state, z, c, and D are low, and reactivity G enables active seed removal, therefore maintaining long-term resilience; (ii) under challenging conditions, i.e. increased damage z and focal range c, the system becomes less stable, and seed removal gradually becomes less functional with decreasing reactivity G; (iii) if reactivity G does not adapt, the system moves closer to a critical transition, and an acute attack can induce a quickly spreading lesion; (iv) in a highly damaged system, reactivity is down-regulated to ensure short-term stability. Nevertheless, high damage induces high levels of dysfunctional glial activity. Insets show levels of damage-inducing (red lines, Gx^2) and damage-repairing (black lines, $x - z$) glial activity as a function of neuron damage x. The steady state is shown by a black circle at the intersection of both lines.

across neurodegenerative diseases is low [28], our model hints at the possibility of common system-level mechanisms which precede the clinical outbreak of the disease, with possible implications for treatment strategies. Fig. 5 shows two stereotypical examples of disease progression in our model framework.

3.1 Alzheimer's disease (AD)

AD is a neurodegenerative disease characterized by the extracellular accumulation of amyloid-β (Aβ) plaques, as well as intracellular accumulation of neurofibrillary tangles consisting of misfolded, hyperphosphorylated tau protein [52]. Next to genetic risk factors [59], lifestyle, cardiovascular disease [88] and meningeal glymphatic system dysfunction [23] also contribute to disease outbreak. In Fig. 5a, the affinity, or selective vulnerability, of a tissue to induce 'seeds' such as amyloid plaques, is set by the seeding rate ν. In contrast, low subthreshold stressors such as lifestyle or glymphatic system dysfunction, are represented by weak distributed frequent stressors on the tissue. Our model simulations show how weak and slow accumulation of subthreshold baseline damage can have huge implications of glial reactivity G, eventually leading to the breakdown of seed removal and a transition from the challenged to the chronic phase.

This is in line with recent genetic studies, which implicate mutations in genes expressed by immune-active cells in the development of late-onset AD – one major risk factor being a mutation of TREM2 (triggering receptor expressed on myeloid cells 2) [54]. TREM2 encodes an innate immune receptor expressed by microglia and is part of an immune checkpoint which controls the activation of Aβ-clearing disease-associated microglia. In particular, functional TREM2 leads to an up-regulated microglial phagocytosis of Aβ plaques early in the disease by activated microglia, but it also increases levels of ApoE (plaque-associated apolipoprotein E) in Aβ plaques, which promotes misfolded protein aggregation [81, 52]. In contrast, TREM2 loss-of-function mice exhibit microglia which appear to be locked in a homeostatic state

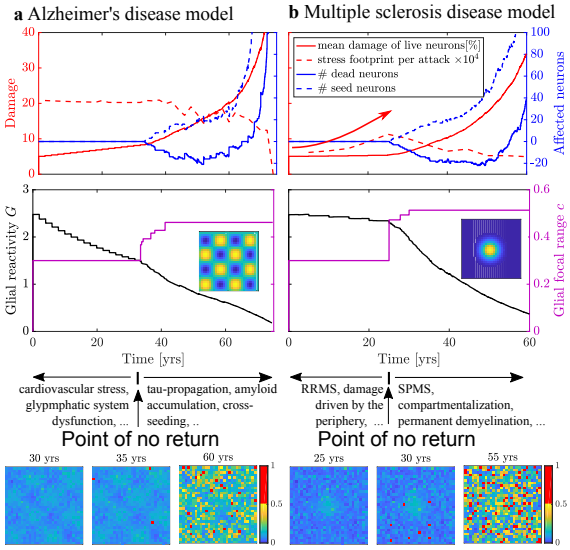

Figure 5: **Neurodegeneration as a result of habituation to subthreshold stressor accumulation.** Left: Frequent, weak distributed stressor across the tissue mimics subthreshold amyloid accumulation due to dysfunctional glymphatic clearance in AD. Gradual adaptation of glial reactivity G to higher mean damage levels across the tissue leads to a breakdown of seed removal. Right: Repeated, stronger stressor at the center of the domain, mimics local, peripherally driven immune cell penetration in the brain parenchyma. Repeated local attacks require an adaptation of the focal range c to maintain short-term stability, leading to a breakdown of seed removal. Prior to this breakdown, the footprint of immune cell attacks increases. In both scenarios, after the point of no return, neuronal death is first offset by seed maintenance, but damage levels increase. Eventually, neuronal death rates increase too. Bottom: Baseline damage levels z prior to, during, and after breakdown of seed removal. Seeds are shown in red. The insets of the graphs of the second row depict the imposed stress pattern.

[81, 96, 54]. Intriguingly, this promotes plaque growth early but not late in the disease. Analogous to the function of reactivity G in our model, TREM2 signaling participates in active seed removal in healthy tissue, but is counterproductive in the chronic phase.

This hints at a possible transition from a challenged but functional phase to a chronic phase, corresponding to the so-called 'cellular phase', in which clearance mechanisms break down [31]. Once the chronic phase is entered, several slow neurodegenerative processes drive disease progression. For instance, dying or damaged neurons release so-called danger-associated molecular patters (DAMPs). These can initiate microglial NLRP3 inflammasome activation, enhance amyloid seeding and promote tau hyperphosphorylation [54, 51]. Experiments also indicate that Aβ plaques disseminate throughout the brain, even though the underlying mechanisms are not yet fully understood [58].

We note that, if generating seeding rates ν are very high, due to excessive stress on neurons with a selective vulnerability to protein aggregation [40] or if average damage levels $\langle z \rangle$ are too high, e.g. in age, then an active removal of seeds may induce collateral damage and become counter-productive. Down-regulation of glial reactivity G, which compromises long-term resilience at the benefit of maintaining short-term resilience, could then be the lesser of two evils.

3.2 Multiple sclerosis (MS)

A hallmark feature of MS is its progression in two sequential disease phases [72]. In the first phase, also referred to as relapse-remitting MS (RRMS), neurodegeneration is driven by immune cells entering the CNS from the periphery through the blood-brain-barrier and attacking myelin sheaths and axons. In the second phase, also referred to as secondary progressive phase (SPMS), neurodegeneration is compartmentalized and chronic. The transition point between these two phases is highly patient-specific and may either happen within a few months, decades or, as in some patients, not occur at all. The reasons for the transition and its high variability are not fully understood [64].

In our model, repeated immune attacks during the relapse-remitting phase of the disease are modeled as focal, repeated stressors (see Fig. 5b). These events raise acute damage levels x (remyelination possible). Depending on how quickly damage is resolved, this affects baseline damage levels z (no remyelination possible). The repeated immune attacks put the reactivity of immune competent cells to the test: As baseline damage levels z increase locally and reactivity G stays high, the 'footprint' of immune attacks increases. In order to avoid a breakdown of short-term stability and collateral damage by acute lesion spread, eventually the focal range c is increased. This leads to a breakdown of seed removal, and slow compartmentalized neurodegenerative processes take over, leading to a transition to the chronic phase (see also Table 1).

The increase of the 'footprint per attack' shows that glial activity persists for a longer time after a peripherally driven immune attack (see Fig. 5b). This is reminiscent of the increasing intensity of RRMS lesions before the transition to SPMS. In contrast, failure to avoid acute lesion spread is equivalent to the development in progressive MS [11] and quickly expanding lesions in fulminant MS [86]. The slow processes in the chronic phase of the disease, which take over after failure of seed removal, are of various origins (see Appendix, Sec. A for details). For instance, myelin debris can inhibit oligodendrocyte differentiation [38]. Also, an impairment of astrocytic glutamate transporter protein expression and glutamate uptake can lead to slow self-enforcing neurodegenerative spreading. Following our model predictions, the point at which glial reactivity G is down-regulated so much that seed-removal breaks down, characterizes the transition from RRMS to SPMS. Postponing the transition from RRMS to SPMS therefore hinges on the careful management of immune attacks and subsequent tissue adaptation.

3.3 Risk factors

Fig.5 highlights the importance of early adaptive changes to subthreshold stressors prior to the outbreak of the disease, thus requiring the consideration of a multidimensional complex system, rather than manipulation of a single signaling pathway (see box). This is consistent with common risk factors. Aging is a major risk factor in AD [105] and MS [39], which affects several parameters in the model presented here. First, baseline damage z increases with age. This may be due to mitochondrial dysfunction, DNA damage and oxidative stress, or maladaptive ion channel redistribution along inflamed axons [39, 106]. Additionally, microglial surveillance functions are down- or dysregulated, corresponding to a widening of the focal range c and a dysregulation of reactivity G. For instance, microglial motility decreases [24], in some brain regions young homeostatic microglial signature is lost [44] and microglia exhibit reduced induced phagocytic activity [105]. In old age, microglia also develop more inflammatory phenotypes [105, 20]. According to the model presented here, this is likely a secondary effect due to increased damage levels x. These induce an overall higher glial activity Gx^2, even if reactivity G is down-regulated (see Tab. 1).

In contrast to the breakdown of seed removal, vulnerability to a transition from the challenged to the primed state may be due to the intracellular accumulation of misfolded proteins, e.g. in AD or Parkinson's disease (PD). In particular, this can influence glial reactions to cell-death D: glial phagocytic function may become up-regulated and negatively affect neighboring neurons [4]; and necrosis of long-term stressed neurons can lead to further inflammation and damage propagation [111]. This can lead to fast domino-

like passing on of neurodegeneration to neighboring tissue, characteristic for the primed state (see Fig. 4). Another possibility is that dying neurons negatively affect baseline damage levels of neighbors, therefore contributing to slow neurodegenerative damage-propagation, characteristic of the chronic state. We also note that vulnerability to the primed state is heightened if glial reactivity is disproportionally upregulated (see Fig. 4), e.g. following immune training from the periphery [109].

3.4 Therapy

Our results suggest postponing the transition from the challenged to the chronic phase as a therapeutic target (see Tab. 1). This transition, which marks the breakdown of maintenance processes, likely precedes the appearance of disease-specific symptoms and clinical diagnosis. The transition may be postponed by keeping the focal range c narrow and glial reactivity G high – which can be summarized as maintaining 'glial fitness'. We note, however, that maintenance of seed-removal and short term resilience become conflicting goals with increasing baseline damage levels, e.g. in stressed tissue or in age. Therefore, G and c need to be carefully managed and adapted. The main goal in the challenged phase is to maintain active seed removal without compromising short-term stability, i.e. avoiding the primed state (see Tab. 1). Possible avenues are the maintenance of the various checkpoint mechanisms of the innate immune system [32], as well maintenance of microglial motility [24]. This becomes increasingly important with age [77]. Warning signs which signal the exhaustion of the challenged state are delayed seed removal (see Fig. 3a) and decreased short-term stability (see Appendix, Fig. 8). Our model therefore suggests the development of diagnostic tools which can probe changes to these dynamic tissue qualities.

Hypothesis:
Glia identify and actively remove damaged but viable neurons (seeds) to prevent slow neurodegenerative feedback processes.
Results: Healthy glial activity is challenged by slow subthreshold stressors and maladaptive immune responses. This affects repair-or-dispose decisions of the neuron-glia unit and leads to (iii) a primed tissue state which amplifies external stressors or (iv) habituation and a breakdown of identification and removal of seeds, resulting in neurodegeneration. In a chronically stressed tissue, maintaining resilience w.r.t. both scenarios represents a conflict of goals.

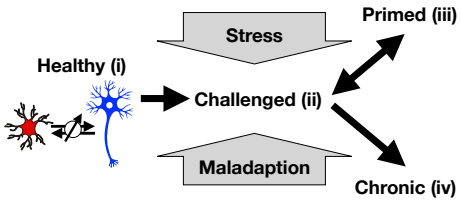

Possible experimental validation: To test our model predictions, the ability of glia to dispose of seeds and to contain activation needs to be measured in the following states (see Table 1): in healthy tissue (state i), after slow subthreshold damage accumulation (state ii), and during neurodegeneration (state iv). The transition to the primed tissue state (iii) can be tested by suppressing the ability of the tissue to habituate to slow damage accumulation, and then test for external stressors amplification.

Active seed removal requires an anti-inflammatory protective tissue reaction to cell death (negative D). The exhaustion of this effect may lead to a primed state and therefore act as an accelerator and facilitator of neurological disease progression, in particular in protein-accumulating diseases. To avoid or postpone this transition, therapeutic interventions need to selectively reinforce the resolution, but not the initiation, of glial reactivity.

In contrast to early disease phases, in which high reactivity G needs to be maintained, our results show that in the chronic phase, active seed removal is dysfunctional, calling for a down-regulation of reactivity G, e.g. using anti-inflammatory treatments. This avoids the vulnerability to collateral damage (see Fig. 4), and slows down feedback processes which drive neurodegeneration. The disease-phase specific approaches

outlined here highlight the importance of maintaining a delicate balance of several processes of neuron-glia crosstalk across different timescales. This is in line with conclusions drawn from failures of clinical trials of AD drugs [18, 34], which call for earlier diagnosis and treatment strategies, as well as the use of more realistic Aβ concentrations for in vitro, cell and animal models.

3.5 Conclusion and Outlook

An experimental verification of the model predictions needs to satisfy several requirements (see box). First, seed removal is a reaction to an innate perturbation, therefore a highly sensitive process. External seed induction must mimic this perturbation. This is especially difficult, as the spontaneous development of pathological processes is poorly reproduced by animal models. In Alzheimer's, the interplay between amyloid plaque deposition, intracellular tangles and dementia is not replicated by any animal model [107]. Second, subthreshold damage accumulation must mimic slow physiological adaptation processes to ageing, cardiovascular dysfunction and glymphatic system dysfunction. It is unlikely that animals with a shorter life span exhibit the same adaptive processes as humans. Finally, the pathology in the model system must develop spontaneously. This significantly constrains experiments, which often hinge on a controlled induction of the disease, and puts the focus on human pathological data.

We argue that animal models provide indispensable insights into mechanisms of brain function. Often, however, they do not replicate the human interplay of these functions sufficiently well to find adequate therapies. Failure to account for the human complexity has been given as one of the reasons for the repeated failure of clinical trials for Alzheimer's [18, 34, 30] and progressive multiple sclerosis [26]. In this light, computational models can provide insights for the interaction of mechanisms across timescales. Nevertheless, we highlight that the model proposed here is a coarse-grained description of neuron-glia crosstalk. Future work needs to extend the model to include other factors which impact tissue maintenance function such as immune communication along the gut-brain axis [103], or the differential activation of astrocytic and microglial phenotypes.

In conclusion, based on existing genetic and experimental reports, we propose a self-consistent computational description of the ambiguous function of neuron-glia crosstalk with a minimal number of parameters. The model is in agreement with current experimental findings for the most common neurodegenerative conditions. We identify stereotypical disease states which are common in health and across several diseases and suggest a state-specific intervention: maintenance of glial fitness, i.e. reactivity and focal range in early, preclinical phases; management of the ability to contain and resolve glial activation after cell death to prevent primed tissue; and reduction of reactivity in the chronic phase of the disease. Specifically, we have shown how failure of the interplay of innate maintenance processes might be at the heart of the onset of the most common neurological diseases. These results highlight the importance of understanding innate and dynamic maintenance processes prior to disease outbreak in the race to find cures for the most common neurological conditions.

4 Material and Methods

4.1 Numerical details

For the simulations, baseline neuronal damages z_n are independently drawn from a log-normal distribution with mean $\langle z \rangle$ and a standard deviation of 50% of the mean. In Fig. 2a, Eq. 1 is solved for 1000 neurons with $\langle z \rangle = 0.05$, averaged over 20 distributions. The seeding rate and slow time scale used in Fig. 2 and 5 are $\nu = 1/(2000\text{yrs}), 1/(500\text{yrs})$ and $\tau_\infty = 25, 50$ years, respectively. The spreading parameter is $M = 10$. 2D simulations in Figs. 4 and 5, were done on a uniform grid of $n \times n$ neurons ($n = 30$). Stressors are modeled by

a local and temporally limited stressor function $f_{\text{ext},n}$ which is added to the right hand side of Eq. 2. For Figs. 4 and 5b, $f_{\text{ext},n} = A(t)e^{-|\mathbf{r}_n - \mathbf{r}_c|^2/(2\sigma^2)}$, where $A(t) = \tilde{A}(1+\tanh((12\text{h}-t)/4\text{h}))/2$ and $\sigma = 3$, $\mathbf{r}_c = (n/2, n/2)$. For 5b, $f_{\text{ext},n} = A(t)(1 + \sin(4\pi(\mathbf{r}_n)_1/n)\sin(4\pi(\mathbf{r}_n)_2/n))/2$. For Fig. 4, $\tilde{A} = 0.25$ and for Fig. 5a and Fig. 5b, $\tilde{A} = 0.1$. In Fig.5, the footprint of each local attack is computed as $\Delta_n = \int_0^\infty x_n \mathrm{d}t - (x_n|_{t=0} + x_n|_{t=\infty})/2$. Attacks increase baseline damage z_n by $\Delta_n/500$ and $\Delta_n/200$, and appear at a rate of 1/(2yrs) and 1/(5yrs) for Figs. 5a and 5b, respectively. In Fig. 5, glial reactivity is constantly adapted such that $4G\langle z\rangle = 1/2$. Glial focal range is adapted such that the maximal eigenvalue of Eq. 2a is not greater than $-0.1/\tau$.

4.2 Seeding parameter S

The seeding equation 1 may be nondimensionalized to obtain

$$\frac{\mathrm{d}z_n}{\mathrm{d}t'} = \frac{1}{\nu\tau_\infty}\sum_{m\in\mathcal{C}_n}[z_m - \theta]_+ + z_{\text{cliff}}\sum_k \delta\left(t' - t'_{k,n}\right), \tag{4}$$

with dimensionless timescale $t' = t\nu$, and where the seeding events $t'_{k,n}$ take place at a rate of one. The early, linear damage propagation is then described by the dimensionless parameter

$$S = \frac{M}{\nu\tau_\infty}. \tag{5}$$

S represents the balance of the spreading strength M, given by the number of elements in $\mathcal{C}_n$ and speed $1/\tau_\infty$, to the rate of independent self-induced seeding events ν.

4.3 Mean field and steady state solutions

The mean field limit of Eqs. 2 is defined by $x_n = x, g_n = g, z_n = z$ constant for all n. The prefactor of the sum in the second term of Eq. 2a was chosen such that the term becomes $\frac{1-c}{1+c}\sum_{m=-\infty}^{\infty} c^{|n-m|} g_m = g$ for $g_n = g$. For subthreshold insults $x < 1$, $g = Gx^2$, the neuronal damage x solves $\tau\frac{\mathrm{d}x}{\mathrm{d}t} = -(x-z) + Gx^2$, with steady states given by $x_\pm = (1 \pm \sqrt{1-4Gz})/(2G)$. Here, x_+ and x_- are the unstable and stable solutions, depicted in Fig. 2b by dashed and solid lines, respectively. The critical point, beyond which no stationary solution exists, is given by $z_{\text{crit}} = 1/(4G)$, as used in Figs. 2b and 3.

5 Acknowledgments

This study was supported by the Max Planck Society (T.T.), German Research Foundation (DFG, SFB CRC-TR-128 to S.B.), the Hertie foundation (mylab, S.B.) and the Joachim Herz foundation (Add-on fellowship, A.N.). The authors are members of the Rhine-Main Neuroscience Network (rmn2). We thank Jochen Roeper and Olga Garaschuk for their insights into possible roles of the mechanism in Parkinson's and Alzheimer's diseases, respectively. A.N. and T.T. thank Andreas Vlachos for valuable discussions about neuroinflammation. A.N. thanks Tatiana Engel for stimulating discussions about about the model framework. A.N. thanks Ana Teles for comments on the manuscript.

A.N., D.B., K.B., S.B., T.T. conceived the study; A.N., D.B. performed the research; A.N. conducted the mathematical analysis and prepared the first draft of the manuscript, A.N., S.B. and T.T. wrote the manuscript, and all authors revised the final manuscript.

References

[1] Larry F. Abbott. Lapicque's introduction of the integrate-and-fire model neuron (1907). *Brain Res. Bull.*, 50(5-6):303–304, 1999.

[2] Larry F. Abbott. Theoretical neuroscience rising. *Neuron*, 60(3):489–495, 2008.

[3] Adriano Aguzzi, Ben A Barres, and Mariko L Bennett. Microglia: scapegoat, saboteur, or something else? *Science*, 339(6116):156–161, 2013.

[4] Pinar Ayata, Ana Badimon, Hayley J Strasburger, Mary Kaye Duff, Sarah E Montgomery, Yong-Hwee E Loh, Anja Ebert, Anna A Pimenova, Brianna R Ramirez, Andrew T Chan, et al. Epigenetic regulation of brain region-specific microglia clearance activity. *Nat. Neurosci.*, 21(8):1049, 2018.

[5] Ben A Barres. The mystery and magic of glia: a perspective on their roles in health and disease. *Neuron*, 60(3):430–440, 2008.

[6] William Bialek, Andrea Cavagna, Irene Giardina, Thierry Mora, Edmondo Silvestri, Massimiliano Viale, and Aleksandra M Walczak. Statistical mechanics for natural flocks of birds. *Proc. Natl. Acad. Sci. U.S.A.*, 109(13):4786–4791, 2012.

[7] William Bialek and Sima Setayeshgar. Physical limits to biochemical signaling. *Proc. Natl. Acad. Sci. U.S.A.*, 102(29):10040–10045, 2005.

[8] Knut Biber, Harald Neumann, Kazuhide Inoue, and Hendrikus WGM Boddeke. Neuronal 'on' and 'off' signals control microglia. *Trends Neurosci.*, 30(11):596–602, 2007.

[9] Michelle L. Block and Jau-Shyong Hong. Microglia and inflammation-mediated neurodegeneration: multiple triggers with a common mechanism. *Prog. Neurobiol.*, 76(2):77–98, 2005.

[10] Michelle L Block, Luigi Zecca, and Jau-Shyong Hong. Microglia-mediated neurotoxicity: uncovering the molecular mechanisms. *Nat. Rev. Neurosci.*, 8(1):57, 2007.

[11] Stephan Bramow, JC Faber-Rod, Christina Jacobsen, A Kutzelnigg, P Patrikios, PS Sorensen, H Lassmann, and Henning Laursen. Fatal neurogenic pulmonary edema in a patient with progressive multiple sclerosis. *Mult. Scler. J.*, 14(5):711–715, 2008.

[12] Johannes Brettschneider, Kelly Del Tredici, Virginia M.-Y. Lee, and John Q. Trojanowski. Spreading of pathology in neurodegenerative diseases: a focus on human studies. *Nat. Rev. Neurosci.*, 16(2):109–120, 2015.

[13] Brad R. S. Broughton, David C. Reutens, and Christopher G. Sobey. Apoptotic mechanisms after cerebral ischemia. *Stroke*, 40(5):e331–e339, 2009.

[14] Guy C Brown and Jonas J Neher. Inflammatory neurodegeneration and mechanisms of microglial killing of neurons. *Mol. Neurobiol.*, 41(2-3):242–247, 2010.

[15] Guy C. Brown and Jonas J. Neher. Microglial phagocytosis of live neurons. *Nat. Rev. Neurosci.*, 15(4):209–216, 2014.

[16] Joshua E Burda and Michael V Sofroniew. Reactive gliosis and the multicellular response to CNS damage and disease. *Neuron*, 81(2):229–248, 2014.

[17] Tyler J Bussian, Asef Aziz, Charlton F Meyer, Barbara L Swenson, Jan M van Deursen, and Darren J Baker. Clearance of senescent glial cells prevents tau-dependent pathology and cognitive decline. *Nature*, 562(7728):578, 2018.

[18] Ewen Callaway. Alzheimer's drugs take a new tack. *Nature News*, 489:7414, 2012.

[19] Ludovico Cantuti-Castelvetri, Dirk Fitzner, Mar Bosch-Queralt, Marie-Theres Weil, Minhui Su, Paromita Sen, Torben Ruhwedel, Miso Mitkovski, George Trendelenburg, Dieter Lütjohann, et al. Defective cholesterol clearance limits remyelination in the aged central nervous system. *Science*, 359(6376):684–688, 2018.

[20] Laura E. Clarke, Shane A. Liddelow, Chandrani Chakraborty, Alexandra E. Münch, Myriam Heiman, and Ben A. Barres. Normal aging induces A1-like astrocyte reactivity. *Proc. Natl. Acad. Sci. USA*, 115(8):E1896–E1905, 2018.

[21] Indra Sethy Coraci, Jens Husemann, Joan W Berman, Christine Hulette, Jennifer H Dufour, Gabriele K Campanella, Andrew D Luster, Samuel C Silverstein, and Joseph B El Khoury. CD36, a class B scavenger receptor, is expressed on microglia in Alzheimer's disease brains and can mediate production of reactive oxygen species in response to β-amyloid fibrils. *Am. J. Pathol.*, 160(1):101–112, 2002.

[22] Melinda Czeh, Pierre Gressens, and Angela M Kaindl. The yin and yang of microglia. *Dev. Neurosci.*, 33(3-4):199–209, 2011.

[23] Sandro Da Mesquita, Antoine Louveau, Andrea Vaccari, Igor Smirnov, R. Chase Cornelison, Kathryn M. Kingsmore, Christian Contarino, Suna Onengut-Gumuscu, Emily Farber, Daniel Raper, et al. Functional aspects of meningeal lymphatics in ageing and Alzheimer's disease. *Nature*, 560(7717):185–191, 2018.

[24] Mausam R Damani, Lian Zhao, Aurora M Fontainhas, Juan Amaral, Robert N Fariss, and Wai T Wong. Age-related alterations in the dynamic behavior of microglia. *Aging cell*, 10(2):263–276, 2011.

[25] Dimitrios Davalos, Jae Kyu Ryu, Mario Merlini, Kim M Baeten, Natacha Le Moan, Mark A Petersen, Thomas J Deerinck, Dimitri S Smirnoff, Catherine Bedard, Hiroyuki Hakozaki, et al. Fibrinogen-induced perivascular microglial clustering is required for the development of axonal damage in neuroinflammation. *Nat. Commun.*, 3:1227, 2012.

[26] Floriana De Angelis, Domenico Plantone, and Jeremy Chataway. Pharmacotherapy in secondary progressive multiple sclerosis: an overview. *CNS drugs*, 32(6):499–526, 2018.

[27] Alix De Calignon, Manuela Polydoro, Marc Suárez-Calvet, Christopher William, David H Adamowicz, Kathy J Kopeikina, Rose Pitstick, Naruhiko Sahara, Karen H Ashe, George A Carlson, et al. Propagation of tau pathology in a model of early Alzheimer's disease. *Neuron*, 73(4):685–697, 2012.

[28] Philip L De Jager, Hyun-Sik Yang, and David A Bennett. Deconstructing and targeting the genomic architecture of human neurodegeneration. *Nat. Neurosci.*, 21(10):1310, 2018.

[29] Maurizio De Pittà, Nicolas Brunel, and Andrea Volterra. Astrocytes: orchestrating synaptic plasticity? *Neuroscience*, 323:43–61, 2016.

[30] Bart De Strooper. Lessons from a failed γ-secretase Alzheimer trial. *Cell*, 159(4):721–726, 2014.

[31] Bart De Strooper and Eric Karran. The cellular phase of Alzheimer's disease. *Cell*, 164(4):603–615, 2016.

[32] Aleksandra Deczkowska, Ido Amit, and Michal Schwartz. Microglial immune checkpoint mechanisms. *Nat. Neurosci.*, 21(6):779–786, 2018.

[33] Francesco Di Virgilio, Stefania Ceruti, Placido Bramanti, and Maria P. Abbracchio. Purinergic signalling in inflammation of the central nervous system. *Trends Neurosci.*, 32(2):79–87, 2009.

[34] Andrew J. Doig, Maria P. del Castillo-Frias, Olivia Berthoumieu, Bogdan Tarus, Jessica Nasica-Labouze, Fabio Sterpone, Phuong H. Nguyen, Nigel M. Hooper, Peter Faller, and Philippe Derreumaux. Why is research on amyloid-β failing to give new drugs for Alzheimer's disease? *ACS Chem. Neurosci.*, 8:1435–1437, 2017.

[35] Mohamed El Behi, Charles Sanson, Corinne Bachelin, Léna Guillot-Noël, Jennifer Fransson, Bruno Stankoff, Elisabeth Maillart, Nadège Sarrazin, Vincent Guillemot, Hervé Abdi, et al. Adaptive human immunity drives remyelination in a mouse model of demyelination. *Brain*, 140(4):967–980, 2017.

[36] Joseph B El Khoury, Kathryn J Moore, Terry K Means, Josephine Leung, Kinya Terada, Michelle Toft, Mason W Freeman, and Andrew D Luster. CD36 mediates the innate host response to β-amyloid. *J. Exp. Med.*, 197(12):1657–1666, 2003.

[37] Susan Elmore. Apoptosis: a review of programmed cell death. *Toxicol. Pathol.*, 35:495–516, 2007.

[38] Robin JM Franklin et al. Regenerating CNS myelin: from mechanisms to experimental medicines. *Nat. Rev. Neurosci.*, 18(12):753, 2017.

[39] Manuel A. Friese, Benjamin Schattling, and Lars Fugger. Mechanisms of neurodegeneration and axonal dysfunction in multiple sclerosis. *Nat. Rev. Neurol.*, 10(4):225–238, 2014.

[40] Hongjun Fu, John Hardy, and Karen E Duff. Selective vulnerability in neurodegenerative diseases. *Nat. Neurosci.*, 21(10):1350–1358, 2018.

[41] Li Gan, Mark R Cookson, Leonard Petrucelli, and Albert R La Spada. Converging pathways in neurodegeneration, from genetics to mechanisms. *Nat. Neurosci.*, 21(10):1300, 2018.

[42] Christian Giaume, Annette Koulakoff, Lisa Roux, David Holcman, and Nathalie Rouach. Astroglial networks: a step further in neuroglial and gliovascular interactions. *Nat. Rev. Neurosci.*, 11(2):87–99, 2010.

[43] Maike Gold and Joseph El Khoury. β-amyloid, microglia, and the inflammasome in Alzheimer's disease. In *Semin. Immunopathol.*, volume 37, pages 607–611. Springer, 2015.

[44] Kathleen Grabert, Tom Michoel, Michail H Karavolos, Sara Clohisey, J Kenneth Baillie, Mark P Stevens, Tom C Freeman, Kim M Summers, and Barry W McColl. Microglial brain region- dependent diversity and selective regional sensitivities to aging. *Nat. Neurosci.*, 19(3):504, 2016.

[45] Jing L Guo and Virginia MY Lee. Cell-to-cell transmission of pathogenic proteins in neurodegenerative diseases. *Nat. Med.*, 20(2):130, 2014.

[46] Annett Halle, Veit Hornung, Gabor C. Petzold, Cameron R. Stewart, Brian G. Monks, Thomas Reinheckel, Katherine A. Fitzgerald, Eicke Latz, Kathryn J. Moore, and Douglas T. Golenbock. The NALP3 inflammasome is involved in the innate immune response to amyloid-β. *Nat. Immunol.*, 9(8):857–865, 2008.

[47] G Jean Harry. Microglia during development and aging. *Pharm. Ther.*, 139(3):313–326, 2013.

[48] Bernhard Hemmer, Martin Kerschensteiner, and Thomas Korn. Role of the innate and adaptive immune responses in the course of multiple sclerosis. *Lancet Neurol.*, 14(4):406–419, 2015.

[49] Michael T Heneka, Monica J Carson, Joseph El Khoury, Gary E Landreth, Frederic Brosseron, Douglas L Feinstein, Andreas H Jacobs, Tony Wyss-Coray, Javier Vitorica, Richard M Ransohoff, et al. Neuroinflammation in Alzheimer's disease. *Lancet Neurol.*, 14(4):388–405, 2015.

[50] Michael T Heneka, Douglas T Golenbock, and Eicke Latz. Innate immunity in Alzheimer's disease. *Nature Immunol.*, 16(3):229, 2015.

[51] Michael T Heneka, Róisín M McManus, and Eicke Latz. Inflammasome signalling in brain function and neurodegenerative disease. *Nat. Rev. Neurosci.*, 19(10):610–621, 2018.

[52] Christopher M Henstridge, Bradley T Hyman, and Tara L Spires-Jones. Beyond the neuron–cellular interactions early in Alzheimer disease pathogenesis. *Nat. Rev. Neurosci.*, 20(2):94–108, 2019.

[53] Frank L. Heppner, Richard M. Ransohoff, and Burkhard Becher. Immune attack: the role of inflammation in Alzheimer's disease. *Nat. Rev. Neurosci.*, 16(6):358–372, 2015.

[54] Suzanne Hickman, Saef Izzy, Pritha Sen, Liza Morsett, and Joseph El Khoury. Microglia in neurodegeneration. *Nat. Neurosci.*, 21(10):1359, 2018.

[55] E. C. Hirsch, T. Breidert, E. Rousselet, S. Hunot, A. Hartmann, and P. P. Michel. The role of glial reaction and inflammation in Parkinson's disease. *Ann. N.Y. Acad. Sci.*, 991(1):214–228, 2003.

[56] Renaud Jolivet, Jay S Coggan, Igor Allaman, and Pierre J Magistretti. Multi-timescale modeling of activity-dependent metabolic coupling in the neuron-glia-vasculature ensemble. *PLoS Comput Biol*, 11(2):e1004036, 2015.

[57] Mathias Jucker and Lary C Walker. Self-propagation of pathogenic protein aggregates in neurodegenerative diseases. *Nature*, 501(7465):45, 2013.

[58] Mathias Jucker and Lary C Walker. Propagation and spread of pathogenic protein assemblies in neurodegenerative diseases. *Nat. Neurosci.*, 21(10):1341, 2018.

[59] Celeste M Karch and Alison M Goate. Alzheimer's disease risk genes and mechanisms of disease pathogenesis. *Biol. Psychiatry*, 77(1):43–51, 2015.

[60] Helmut Kettenmann, Uwe-Karsten Hanisch, Mami Noda, and Alexei Verkhratsky. Physiology of microglia. *Physiol. Rev.*, 91(2):461–553, 2011.

[61] Baljit S. Khakh and Michael V. Sofroniew. Diversity of astrocyte functions and phenotypes in neural circuits. *Nat. Neurosci.*, 18(7):942–952, 2015.

[62] Thomas Korn, Tim Magnus, and Stefan Jung. Autoantigen specific T cells inhibit glutamate uptake in astrocytes by decreasing expression of astrocytic glutamate transporter GLAST: a mechanism mediated by tumor necrosis factor-α. *The FASEB journal*, 19(13):1878–1880, 2005.

[63] Georg W. Kreutzberg. Microglia: a sensor for pathological events in the CNS. *Trends Neurosci.*, 19(8):312–318, 1996.

[64] Catherine Larochelle, Timo Uphaus, Alexandre Prat, and Frauke Zipp. Secondary progression in multiple sclerosis: neuronal exhaustion or distinct pathology? *Trends Neurosci.*, 39(5):325–339, 2016.

[65] Hosuk Sean Lee, Andrea Ghetti, António Pinto-Duarte, Xin Wang, Gustavo Dziewczapolski, Francesco Galimi, Salvador Huitron-Resendiz, Juan C Piña-Crespo, Amanda J Roberts, Inder M Verma, et al. Astrocytes contribute to gamma oscillations and recognition memory. *Proc. Natl. Acad. Sci. U.S.A.*, 111(32):E3343–E3352, 2014.

[66] Roland S. Liblau, Daniel Gonzalez-Dunia, Heinz Wiendl, and Frauke Zipp. Neurons as targets for T cells in the nervous system. *Trends Neurosci.*, 36(6):315–324, 2013.

[67] Shane A. Liddelow, Kevin A. Guttenplan, Laura E. Clarke, Frederick C. Bennett, Christopher J. Bohlen, Lucas Schirmer, Mariko L. Bennett, Alexandra E. Münch, Won-Suk Chung, Todd C. Peterson, et al. Neurotoxic reactive astrocytes are induced by activated microglia. *Nature*, 541(7638):481–487, 2017.

[68] Jane H-C Lin, Nanhong Lou, Ning Kang, Takahiro Takano, Furong Hu, Xiaoning Han, Qiwu Xu, Ditte Lovatt, Arnulfo Torres, Klaus Willecke, et al. A central role of connexin 43 in hypoxic preconditioning. *J. Neurosci.*, 28(3):681–695, 2008.

[69] Jane H.-C. Lin, Helga Weigel, Maria Luisa Cotrina, Shujun Liu, Earl Bueno, Anker J. Hansen, Thomas W. Hansen, Steven Goldman, and Maiken Nedergaard. Gap-junction-mediated propagation and amplification of cell injury. *Nat. Neurosci.*, 1(6):494–500, 1998.

[70] Fred D. Lublin, Stephen C. Reingold, Jeffrey A. Cohen, Gary R. Cutter, Per Soelberg Sørensen, Alan J. Thompson, Jerry S. Wolinsky, Laura J. Balcer, Brenda Banwell, Frederik Barkhof, et al. Defining the clinical course of multiple sclerosis. The 2013 revisions. *Neurology*, 83(3):278–286, 2014.

[71] Dirk Luchtman, René Gollan, Erik Ellwardt, Jérôme Birkenstock, Kerstin Robohm, Volker Siffrin, and Frauke Zipp. In vivo and in vitro effects of multiple sclerosis immunomodulatory therapeutics on glutamatergic excitotoxicity. *J. Neurochem.*, 136:971–980, 2016.

[72] Don H Mahad, Bruce D Trapp, and Hans Lassmann. Pathological mechanisms in progressive multiple sclerosis. *Lancet Neurol.*, 14(2):183–193, 2015.

[73] Nicholas J. Maragakis and Jeffrey D. Rothstein. Mechanisms of disease: astrocytes in neurodegenerative disease. *Nat. Rev. Neurol.*, 2(12):679–689, 2006.

[74] K. Mitosek-Szewczyk, G. Sulkowski, Z. Stelmasiak, and L. Strużyńska. Expression of glutamate transporters glt-1 and glast in different regions of rat brain during the course of experimental autoimmune encephalomyelitis. *Neuroscience*, 155(1):45–52, 2008.

[75] Taizen Nakase, Shinji Fushiki, and Christian CG Naus. Astrocytic gap junctions composed of connexin 43 reduce apoptotic neuronal damage in cerebral ischemia. *Stroke*, 34(8):1987–1993, 2003.

[76] I. Napoli and H. Neumann. Microglial clearance function in health and disease. *Neuroscience*, 158(3):1030–1038, 2009.

[77] Raffaella Nativio, Greg Donahue, Amit Berson, Yemin Lan, Alexandre Amlie-Wolf, Ferit Tuzer, Jon B. Toledo, Sager J. Gosai, Brian D. Gregory, Claudio Torres, et al. Dysregulation of the epigenetic landscape of normal aging in Alzheimer's disease. *Nat. Neurosci.*, 21(4):497–505, 2018.

[78] Klaus-Armin Nave. Myelination and support of axonal integrity by glia. *Nature*, 468(7321):244–252, 2010.

[79] H. Neumann, M. R. Kotter, and R. J. M. Franklin. Debris clearance by microglia: an essential link between degeneration and regeneration. *Brain*, 132(2):288–295, 2008.

[80] Axel Nimmerjahn, Frank Kirchhoff, and Fritjof Helmchen. Resting microglial cells are highly dynamic surveillants of brain parenchyma in vivo. *Science*, 308:1314–1318, 2005.

[81] Samira Parhizkar, Thomas Arzberger, Matthias Brendel, Gernot Kleinberger, Maximilian Deussing, Carola Focke, Brigitte Nuscher, Monica Xiong, Alireza Ghasemigharagoz, Natalie Katzmarski, et al. Loss of TREM2 function increases amyloid seeding but reduces plaque-associated apoe. *Nat. Neurosci.*, 22(2):191–204, 2019.

[82] Geraldine T Petr, Yan Sun, Natalie M Frederick, Yun Zhou, Sameer C Dhamne, Mustafa Q Hameed, Clive Miranda, Edward A Bedoya, Kathryn D Fischer, Wencke Armsen, et al. Conditional deletion of the glutamate transporter GLT-1 reveals that astrocytic GLT-1 protects against fatal epilepsy while neuronal GLT-1 contributes significantly to glutamate uptake into synaptosomes. *J. Neurosci.*, 35(13):5187–5201, 2015.

[83] Ivan K. H. Poon, Christopher D. Lucas, Adriano G. Rossi, and Kodi S. Ravichandran. Apoptotic cell clearance: basic biology and therapeutic potential. *Nat. Rev. Immunol.*, 14(3):166–180, 2014.

[84] Richard M. Ransohoff. A polarizing question: do M1 and M2 microglia exist? *Nat. Neurosci.*, 19(8):987–991, 2016.

[85] Khalil S Rawji, Janson Kappen, Weiwen Tang, Wulin Teo, Jason R Plemel, Peter K Stys, and V Wee Yong. Deficient surveillance and phagocytic activity of myeloid cells within demyelinated lesions in ageing mice visualized by ex vivo live multiphoton imaging. *J. Neurosci.*, pages 2341–17, 2018.

[86] Mohammad Rohani and Shadi Ghourchian. Fulminant multiple sclerosis (MS). *Neurol. Sci.*, 32(953), 2011.

[87] Michael W. Salter and Beth Stevens. Microglia emerge as central players in brain disease. *Nat. Med.*, 23(9):1018–1027, 2017.

[88] Cláudia Y. Santos, Peter J. Snyder, Wen-Chih Wu, Mia Zhang, Ana Echeverria, and Jessica Alber. Pathophysiologic relationship between Alzheimer's disease, cerebrovascular disease, and cardiovascular risk: a review and synthesis. *Alzheimers Dement. (AMST)*, 7:69–87, 2017.

[89] John Savill and Valerie Fadok. Corpse clearance defines the meaning of cell death. *Nature*, 407(6805):784–788, 2000.

[90] Benjamin Schattling, Jan Broder Engler, Constantin Volkmann, Nicola Rothammer, Marcel S Woo, Meike Petersen, Iris Winkler, Max Kaufmann, Sina C Rosenkranz, Anna Fejtova, et al. Bassoon proteinopathy drives neurodegeneration in multiple sclerosis. *Nat. Neurosci.*, page 1, 2019.

[91] Marten Scheffer, Stephen R. Carpenter, Timothy M. Lenton, Jordi Bascompte, William Brock, Vasilis Dakos, Johan van de Koppel, Ingrid A. van de Leemput, Simon A. Levin, Egbert H. van Nes, et al. Anticipating critical transitions. *Science*, 338:344–348, 2012.

[92] Frederick J. Sheedy, Alena Grebe, Katey J. Rayner, Parisa Kalantari, Bhama Ramkhelawon, Susan B. Carpenter, Christine E. Becker, Hasini N. Ediriweera, Adam E. Mullick, Douglas T. Golenbock, et al. CD36 coordinates NLRP3 inflammasome activation by facilitating intracellular nucleation of soluble ligands into particulate ligands in sterile inflammation. *Nat. Immunol.*, 14(8):812–820, 2013.

[93] Yongdae Shin and Clifford P Brangwynne. Liquid phase condensation in cell physiology and disease. *Science*, 357(6357):eaaf4382, 2017.

[94] Volker Siffrin, Helena Radbruch, Robert Glumm, Raluca Niesner, Magdalena Paterka, Josephine Herz, Tina Leuenberger, Sabrina M. Lehmann, Sarah Luenstedt, Jan Leo Rinnenthal, et al. In vivo imaging of partially reversible th17 cell-induced neuronal dysfunction in the course of encephalomyelitis. *Immunity*, 33(3):424–436, 2010.

[95] Michael V Sofroniew and Harry V Vinters. Astrocytes: biology and pathology. *Acta Neuropathol.*, 119(1):7–35, 2010.

[96] Wilbur M Song, Satoru Joshita, Yingyue Zhou, Tyler K Ulland, Susan Gilfillan, and Marco Colonna. Humanized TREM2 mice reveal microglia-intrinsic and-extrinsic effects of R47H polymorphism. *J. Exp. Med.*, 215(3):745–760, 2018.

[97] Elizabeth E. Spangenberg, Rafael J. Lee, Allison R. Najafi, Rachel A. Rice, Monica R. P. Elmore, Mathew Blurton-Jones, Brian L. West, and Kim N. Green. Eliminating microglia in Alzheimer's mice prevents neuronal loss without modulating amyloid-β pathology. *Brain*, 139:1265–1281, 2016.

[98] Krista J Spiller, Clark R Restrepo, Tahiyana Khan, Myrna A Dominique, Terry C Fang, Rebecca G Canter, Christopher J Roberts, Kelly R Miller, Richard M Ransohoff, John Q Trojanowski, et al. Microglia-mediated recovery from ALS-relevant motor neuron degeneration in a mouse model of TDP-43 proteinopathy. *Nat. Neurosci.*, 21(3):329, 2018.

[99] Nick Stence, Marc Waite, and Michael E. Dailey. Dynamics of microglial activation: a confocal time-lapse analysis in hippocampal slices. *Glia*, 33:256–266, 2001.

[100] Alexander H Stephan, Ben A Barres, and Beth Stevens. The complement system: an unexpected role in synaptic pruning during development and disease. *Annu. Rev. Neurosci.*, 35:369–389, 2012.

[101] D. James Surmeier, José A. Obeso, and Glenda M. Halliday. Selective neuronal vulnerability in Parkinson disease. *Nat. Rev. Neurosci.*, 18(2):101–113, 2017.

[102] Carmen Venegas, Sathish Kumar, Bernardo S. Franklin, Tobias Dierkes, Rebecca Brinkschulte, Dario Tejera, Ana Vieira-Saecker, Stephanie Schwartz, Francesco Santarelli, Markus P. Kummer, et al. Microglia-derived ASC specks cross-seed amyloid-β in Alzheimer's disease. *Nature*, 552(7685):355–361, 2017.

[103] Nicholas M Vogt, Robert L Kerby, Kimberly A Dill-McFarland, Sandra J Harding, Andrew P Merluzzi, Sterling C Johnson, Cynthia M Carlsson, Sanjay Asthana, Henrik Zetterberg, Kaj Blennow, et al. Gut microbiome alterations in Alzheimer's disease. *Sci. Rep.*, 7(1):13537, 2017.

[104] Rommy Von Bernhardi. Glial cell dysregulation: a new perspective on Alzheimer disease. *Neurotox Res.*, 12(4):215–232, 2007.

[105] Rommy Von Bernhardi, Laura Eugenín-von Bernhardi, and Jaime Eugenín. Microglial cell dysregulation in brain aging and neurodegeneration. *Front. Aging Neurosci.*, 7:124, 2015.

[106] Rommy Von Bernhardi, Juan E Tichauer, and Jaime Eugenín. Aging-dependent changes of microglial cells and their relevance for neurodegenerative disorders. *J. Neurochem.*, 112(5):1099–1114, 2010.

[107] Lary C Walker and Mathias Jucker. The exceptional vulnerability of humans to Alzheimer's disease. *Trends Mol. Med.*, 23(6):534–545, 2017.

[108] Johannes Weickenmeier, Ellen Kuhl, and Alain Goriely. Multiphysics of prionlike diseases: Progression and atrophy. *Phys. Rev. Lett.*, 121:158101, Oct 2018.

[109] Ann-Christin Wendeln, Karoline Degenhardt, Lalit Kaurani, Michael Gertig, Thomas Ulas, Gaurav Jain, Jessica Wagner, Lisa M Häsler, Katleen Wild, Angelos Skodras, et al. Innate immune memory in the brain shapes neurological disease hallmarks. *Nature*, 556(7701):332, 2018.

[110] Yochai Wolf, Simon Yona, Ki-Wook Kim, and Steffen Jung. Microglia, seen from the CX3CR1 angle. *Front. Cell. Neurosci.*, 7:26, 2013.

[111] Junying Yuan, Palak Amin, and Dimitry Ofengeim. Necroptosis and RIPK1-mediated neuroinflammation in CNS diseases. *Nat. Rev. Neurosci.*, 20(1):19–33, 2018.

[112] Jennifer L Zamanian, Lijun Xu, Lynette C Foo, Navid Nouri, Lu Zhou, Rona G Giffard, and Ben A Barres. Genomic analysis of reactive astrogliosis. *J. Neurosci.*, 32(18):6391–6410, 2012.

Appendix A Biological processes of neuron-glia crosstalk across timescales

In Fig. 1 of the main manuscript, we classify neuron-glia interactions into five classes. In Supplementary Fig. 6, we show at which time scale these interactions act. We distinguish between neuron-glia interactions which equilibrate in the timescale of hours to days, and slow processes, which drive neurodegeneration over the timescale of months to years.

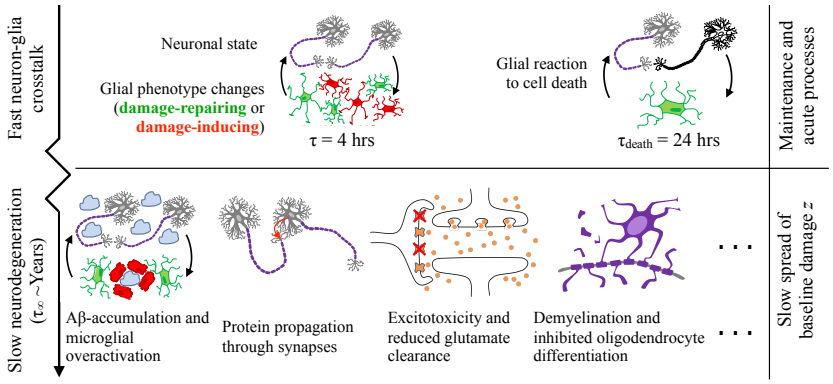

Figure 6: **Neuron-glia crosstalk across timescales.** Top: On the timescale of hours, glia react differentially to neuronal damage: They provide neurotrophic support and repair, but can also induce damage. Glia also quickly react to neuronal cell death and induce a response which decays with timescale τ_{death}. Bottom: At the timescale of years, slow age-, lifestyle- and disease-specific processes induce permanent neuronal damage, depicted by prototypical processes of the most common neurological diseases. With '...' we indicate that only a selection is shown here.

A.1 Details of fast processes of neuron-glia crosstalk

In this section, we provide further detail for the biological processes modeled in Eq. 2 of the main manuscript.

Damage-repairing housekeeping functions Glia, the helper cells of the brain, play a crucial role in maintaining homeostasis, and in driving and resolving inflammation in the brain. Both microglia [63, 8, 110, 60, 84] and astrocytes [112, 61] exhibit differential and multidimensional activity patterns, which depend – among other factors – on the neuronal state. For instance, microglia provide neurotrophic support [51] and surveil the tissue [80]. Microglial activity is suppressed by so-called neuronal 'Off'-signals, allowing for a regulation of sensing and housekeeping functions [8, 110, 60]. These signals are mediated by receptor-ligand interactions such as CX3CL1 and CD200 signaling [54, 51].

These homeostatic effects are included in the first term $x - z$ on the right-hand-side of Eq. 2a of the main manuscript. Note that we assume that the strength of repair functions increases proportionally with the amount of neuronal damage.

Damage-inducing glial functions Glial activation is, however, a double-edged sword and can, under certain conditions, induce neuronal damage [22]. For instance, neurons may directly recruit microglia by releasing ATP, facilitating phagocytosis [47] or by releasing glutamate, which triggers microglial TNFα

release [60]. Astrocytes respond to infections, trauma or inflammation by a process known as reactive astrogliosis, characterized by an increased production of pro-inflammatory cytokines such as IL-1β and TNF-α, and reactive oxygen species (ROS) [95]. Reactive astrocytes may also play an important role in inducing complement-mediated synapse elimination, which in many neurodegenerative diseases precedes, and might even drive, neuronal loss [100]. Overactivated microglia can induce the transition of nearby astrocytes to a highly neurotoxic phenotype, causing widespread damage to the tissue [67]. Microglia can also remove stressed-but-viable neurons as a response to so-called 'eat-me-signals' [14, 15].

The departure from the neuroprotective tissue reaction due to damage-inducing glial activity is modeled by the second term g_m on the right hand side of Eq. 2a and Eq.2b of the main manuscript.

Spatial effects and focal range One key ingredient of the model is that glial activity may not be perfectly precise in space, and may therefore affect neighboring parts of the tissue. This can happen through different pathways: For instance, pro-inflammatory phenotypes in neighboring cells can be induced by cytokine diffusion. Microglia migrate to regions of insult [99] and form clusters as a reaction to blood-derived fibrinogen [25]. Therefore, inhibition of microglial motility [24] can lead to a loss of specificity and loss of precision. Also, astrocytic gap junction communication has been shown to play a role in spatial propagation of cell injury [69], and neuroprotection in ischemia [75, 68] (see [42] for a review).

These spatial effects are modeled in the sum in Eq. 2a of the main manuscript.

Glial reactions to cell death Microglia clear neuronal debris [63], secrete anti-inflammatory cytokines and minimize damage to surrounding cells [89, 37, 13]. An epigenetically mediated dysregulation of this tightly controlled clearance function can lead to damage in healthy neurons [4]. Also following necrosis [83], in age [79], and in neurodegenerative diseases [76] phagocytosis is reduced or can induce pro-inflammatory reactions via ATP released from dying neurons [33].

The resolution of inflammation following cell death, or its pro-inflammatory tissue reactions, are modeled by the exponential decay term in Eq. 2b.

A.2 Details of slow neurodegenerative processes

In this section, we provide further detail for the slow processes in different diseases which form vicious feedback loops and drive disease progression. These processes are modeled in Eq. 1 of the main manuscript.

Note how despite their different mechanisms, these processes have the following common key properties: First, the respective neuronal damage caused is permanent, i.e. it cannot be repaired by intracellular or glial functions. Second, once the damage exceeds a certain threshold, it spreads through the tissue. Finally, the processes involved are slow, and the permanent damage caused in the initial stages is not severe enough to kill individual neurons.

Protein accumulating diseases The accumulation of proteins in insoluble aggregates is a hallmark of Alzheimer's disease (AD) and Parkinson's disease (PD). It is thought that seeds recruit their soluble counterparts in living cells, therefore establishing a self-driven process. There is also evidence that neurodegeneration and glial reaction to it form a positive feedback [9, 10].

In vitro studies for AD show that Aβ induces inflammatory microglial responses [46, 92] and primes microglia for a secondary stimulus [53]. These activated glial cells appear before the first structural changes in the tissue [49]. Initially, the immune response amplifies the glial clearance abilities on early stages of aggregation [50]. However, prolonged exposure to excessive concentrations of proteins causes chronic inflammation. Overactivated microglia and reactive astrocytes then express neurotoxic factors [43, 36, 21] and impaired Aβ clearance [105] and lose their cleaning abilities [97]. This winds up the protein aggregation

[31] and compromises the inflammation resilience in a vicious feed-back loop. In AD, the feedback has recently been linked to microglia-derived ASC specks, which act as an inflammation-driven cross-seed for Aβ pathology [102].

In AD, these processes extend the 'amyloid cascade hypothesis', where Aβ is seen as the main driving force of the disease. In particular, it has been proposed that AD transitions from a reversible disease course to an irreversible chronic autonomous cellular response. In this phase, disease progression no longer depends on aggregated proteins which trigger the initial response, but on glial chronic inflammation [104, 31].

Similarly, PD may progress when the initial cause of neurodegeneration has disappeared [55], pointing to a self-promoting mechanism within the brain tissue. Parkinson's disease is characterized by the intracellular accumulation of α-synunclein protein in dopaminergic neurons of the substantia nigra. Damage spreading occurs if α-synunclein take-up by microglia induces inflammasome activation which in turn leads to α-synunclein truncation and accumulation [51]. Slow damage spread has also been reported in ALS and metastatic cancer [58].

Additionally, there is evidence that misfolded proteins, in particular tau and α-synunclein, can propagate from neuron to neuron [27, 12, 101] in a 'prion-like' manner [58]. This self-propagating seeding process may spread via synaptic connections [27, 45] or other mechanisms [12].

Multiple sclerosis In MS, immune cells penetrate the brain, demyelinate neurons [70] and induce excitotoxic insults [94, 66]. Several self-propagating processes can induce a vicious neurodegenerative cycle. First, in acute MS lesions, the transporter protein levels GLT-1 and GLAST are dysregulated and therefore impaired in their ability to take up glutamate [62, 74]. This is also seen in amyotrophic lateral sclerosis (ALS) [73]. This reduction in the astrocytic glutamate uptake [82] can exacerbate the toxic increases of intracellular calcium [71] following T-cell attacks in MS. This means that the tissue becomes increasingly vulnerable to excitotoxicity and external stress.

Second, with age and in disease, glial processes can reduce remyelination of neuronal axons. This may be a consequence of impaired myelin clearance from an initial insult due to reduced motility, surveillance, and phagocytic activity of activated microglia with age [85]. In MS, impaired myelin debris clearance can then lead to cholesterol crystallisation, inflammasome activation and a maladaptive immune response [19, 38]. Importantly, reduced myelin debris clearance, and the resulting myelin debris in the tissue, inhibits oligodendrocyte progenitor cell differentiation into oligodendrocytes [38], further aggravating the problem. Additionally, in MS, regulatory lymphocytes, which act through crosstalk with microglia [35], are less effective in inducing remyelination. Also, chronic inflammation and microglial activation, and increasing neuronal oxidative stress and damage of the axon-glia unit, can lead to a self-perpetuating vicious cycle [48, 78]. Recent studies even point at the possibility that decoupled pathological protein-propagation contributes to this vicious cycle in progressive MS , although research is still at an early stage [90].

Appendix B Mathematical analysis

B.1 Focal range c

The interplay between glial reactivity G, focal range c determines the tissue reaction to neuronal damage. It therefore determines whether seed removal is functional or not. In Fig. 7, the population effect of four configurations of G and c is shown as an example. In the following, we study the behavior of Eq. 2a of the main manuscript in the limit of very narrow and very wide focal ranges.

If the glial focal range is very narrow, $c \to 0$, then $\frac{1-c}{1+c}\sum_{m=-\infty}^{\infty} c^{|n-m|} g_m \to g_n$, and we obtain indepen-

dent ordinary differential equations for all n:

$$\tau \frac{\mathrm{d}x_n}{\mathrm{d}t} = -(x_n - z_n) + g_n. \tag{6}$$

The results of the mean field section then hold individually for each neuron.

If the glial focal range is very wide, $c \to 1$, we map the discrete values of n onto the spatial variable $\eta = \Delta \cdot n$ with $\Delta = -\log c$. As $c \to 1$, Δ decreases to zero, allowing us to define continuous state variables $x(\eta), g(\eta), z(\eta)$. The sum in the second term of Eq. 2a becomes

$$\begin{aligned}
\frac{1-c}{1+c} \sum_{m=-\infty}^{\infty} c^{|n-m|} g_m &= \frac{1-c}{1+c} \sum_{m=-\infty}^{\infty} e^{-\Delta|n-m|} g_m \\
&\xrightarrow{c\to 1} \frac{\Delta}{2} \sum_{m=-\infty}^{\infty} e^{-\Delta|n-m|} g_m \\
&\xrightarrow{\Delta\to 0} \frac{1}{2} \int_{-\infty}^{\infty} e^{-|\eta-\eta'|} g(\eta') \mathrm{d}\eta',
\end{aligned}$$

where we used that $\frac{1-c}{1+c} \to \frac{\Delta}{2} + O(c-1)^3$ as $c \to 1$. Eq. 2a then becomes an integral equation

$$\tau \frac{\partial x}{\partial t} = -(x - z) + \frac{1}{2} \int_{-\infty}^{\infty} e^{-|\eta-\eta'|} g(\eta') \mathrm{d}\eta'. \tag{7}$$

Therefore, for highly imprecise glial reactivities the characteristic length scale is Δ and the influence of one neuron on another decays exponentially on that length scale. This can be observed in Fig. 3 and in the snapshots of Fig.10.

B.2 Stability analysis

In Fig. 3 of the main manuscript, subthreshold properties of the system were studied for different mean damage levels $\langle z \rangle$ and different reactivities G. Here, we investigate the critical point for a single neuron. We do this by considering the nondimensionalized form of Eq. 2 of the main manuscript for $x_n < 1$

$$\tau \frac{\mathrm{d}h_n}{\mathrm{d}t} = -\left(h_n - \frac{H_n}{4}\right) + \frac{1-c}{1+c} \sum_m c^{|n-m|} h_m^2, \tag{8}$$

with $h_n = G x_n$ and $H_n = 4G z_n$. This allows us to plot one stability diagram in (H, c)-space in Appendix Fig. 8.

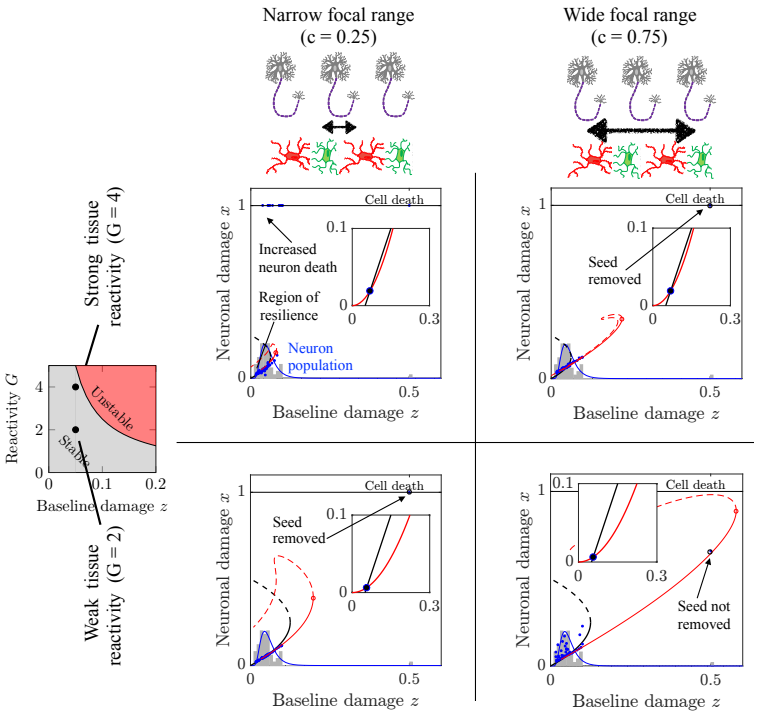

Figure 7: **Functional tissue resilience requires tuning between focal range c and tissue reactivity G.** Black solid and dashed lines represent stable und unstable steady states in the mean field limit. Red solid and dashed lines represent stable und unstable steady states of one neuron for a given (z_n)-distribution. Blue dots represent a population of 200 neurons, taken from a log-normal distribution (blue lines). Grey bars represent the histogram of their (z_n)-distribution. Note that some neurons cross the death threshold at unity. For a narrow focal range ($c = 0.25$), neurons react independently of each other (see left column). For a wide focal range ($c = 0.75$), population effects allow for regional compensation of locally elevated stress levels (see top right), but also of rescue of neuronal seeds, if the reactivity G is attenuated (see bottom right). Red and black lines of the insets show mean field damage inducing and damage reducing glial effects Gx^2 and $x - z$, respectively, as a function of neuronal damage x.

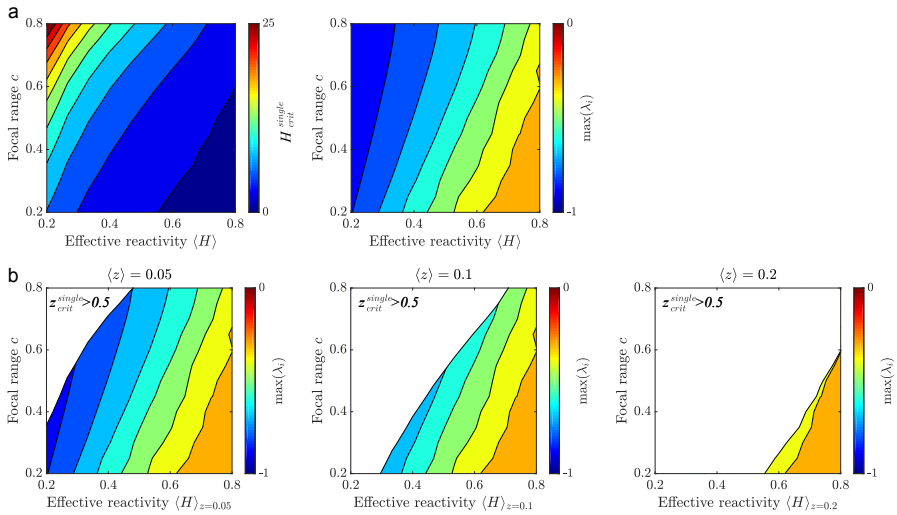

Figure 8: **Short-term stability and seed removal.** Analysis of Eq. 8 as a function of effective population reactivity $\langle H \rangle$ and focal range c for a one-dimensional configuration. **a** Left: seed removal threshold $H_{\text{crit}}^{\text{single}}$ for a single neuron. Here, we studied the stability of the first neuron in a system of 25 neurons, and the resulting $H_{\text{crit}}^{\text{single}}$ was obtained by averaging over 50 (h_n)-distributions. Right: Highest eigenvalue λ_i. Higher eigenvalues indicate reduced short-term stability. **b**, Stability analysis from **a**, applied to three concrete values of z. Varying H then stands for varying glial reactivity G. White areas indicate parameter ranges for which seed removal fails, i.e. $z_{\text{crit}}^{\text{single}} > 0.5$. As baseline damage increases, allowed parameter ranges become more constrained and less stable (higher eigenvalues). With increasing population-wide baseline damage levels $\langle z \rangle$, active seed removal and short-term tissue stability become conflicting goals: effective damage $\langle H \rangle$ needs to be higher and focal range c needs to be narrow in order to ensure active seed removal. This pushes the system into increasingly unstable parameter ranges.

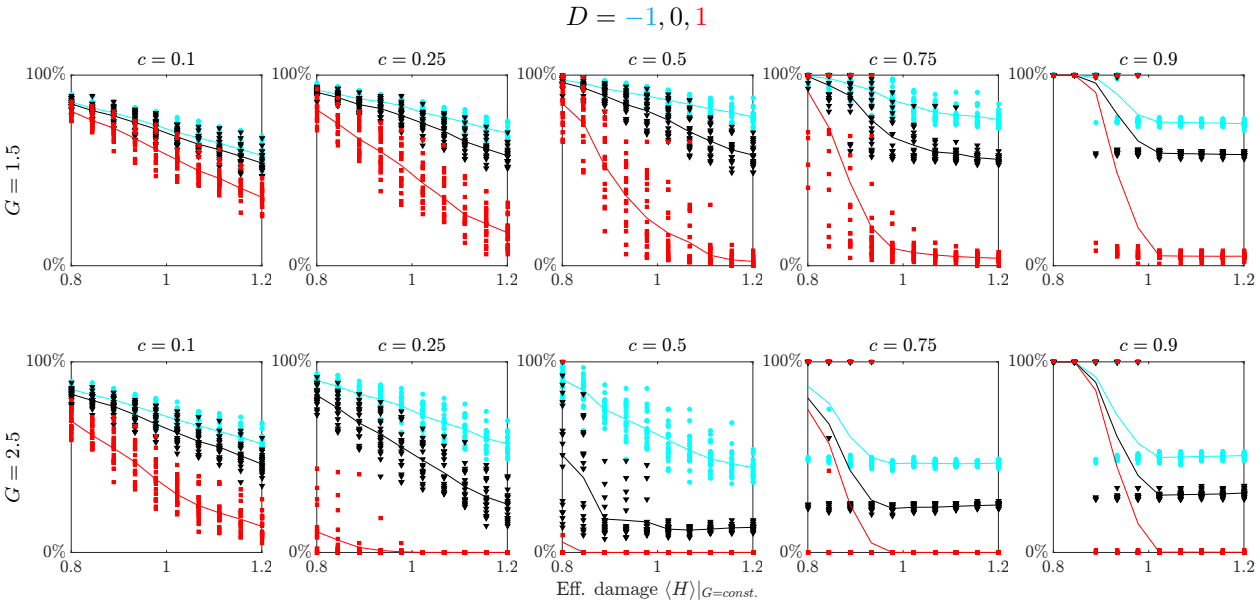

Figure 9: **Critical transitions as in Fig. 4b of the main manuscript.** Survival rate for different strengths of glial reactivity G for different levels of glial focal range c, plotted as a function of the effective damage parameter $\langle H \rangle|_{G=const.}$. Simulations with anti-inflammatory, neutral or pro-inflammatory glial reaction to cell death ($D = -1, 0, 1$) are represented by cyan, black and red lines, respectively. Each symbol represents distribution of baseline damage levels (z_n), and solid lines represent mean values. Parameters: $N = 100$ in a periodic domain, $t_{\max} = 10$ days, 20 runs per parameter set. Systems with a wide focal range ($c \to 1$) exhibit step-like transitions, for which all neurons survive until the critical point is reached, beyond which a steep decrease in survival rates is seen. In contrast, for narrow focal ranges ($c \to 0$), each neuron-glia unit reacts separately to the individual stress levels of the neuron, therefore allowing for a gradual decline of survival rates. Protective glial reactions to cell death ($D = -1$) can act as a barrier for the spread of damage and glial dysregulation and stabilize neuron loss after crossing the critical transition. If glial protective effects to neuronal cell death are attenuated ($D = 0$) or become toxic ($D = 1$), then the death of the first neuron sets off a domino-like knock-on effect that can lead to the death of large parts of the population. Tissue with intermediate focal range (e.g. $c = 0.5$) is particularly vulnerable to this effect, because local stress by a dying neuron fully acts on the neighboring neuron, and is not distributed across the tissue. This means that even though the system is stable locally, i.e. small perturbations to the damage levels can be compensated for, it is not stable with respect to the impact of one dying neuron, which sets off a propagating lesion.

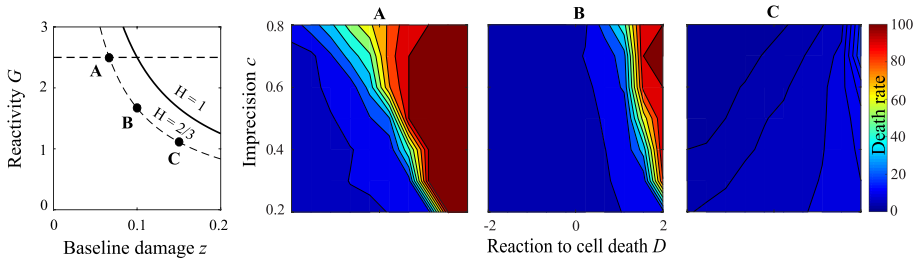

(a) Death rate of a subthreshold stable tissue following an external attack for different baseline damage levels z, as a function of glial reaction to cell death D and focal range c, for effective reactivity $\langle H \rangle = 4G\langle z \rangle = 2/3$.

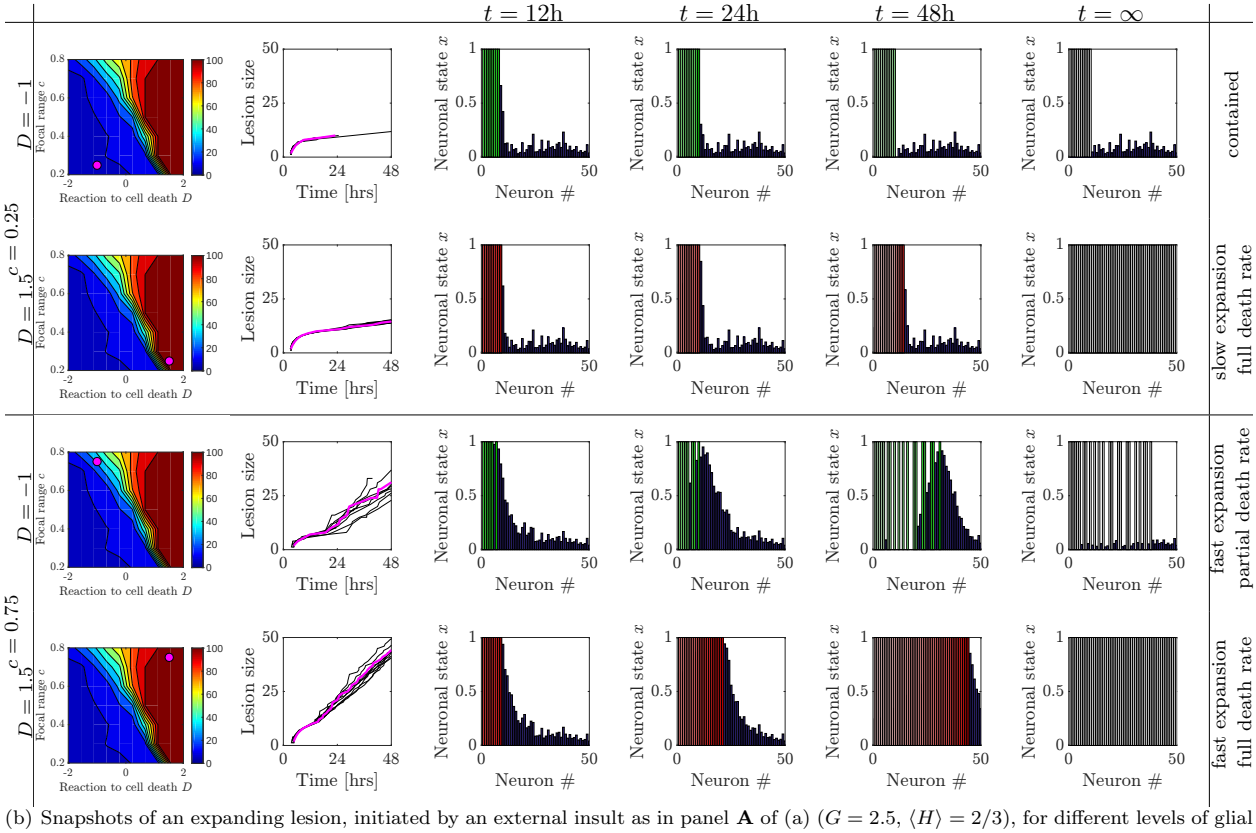

(b) Snapshots of an expanding lesion, initiated by an external insult as in panel **A** of (a) ($G = 2.5$, $\langle H \rangle = 2/3$), for different levels of glial focal range c and glial reaction to cell death D. Magenta circles in the plots of the first column depict the chosen parameter set. The colorscale in the first column represents the death rate, as in (a). The second column depicts lesion front paths for 10 (z_n)-distributions. The snapshot panels ($t = 12\text{h}, 24\text{h}, \ldots$) show neuronal damage values x_n for the path represented by the magenta line. Each bar represents one neuron. Blue bars represent amount of damage of alive neurons. Bars that reach 1 are dead neurons. Levels of red and green represents the level of inflammatory and anti-inflammatory glial reaction to neuronal cell death, respectively.

Figure 10: **Analysis of primed tissue.** Impact of an acute attack on a stable one-dimensional tissue with 100 neurons. Here, the stressor function is $f_{\text{ext},n} = e^{-t/\tau_{\text{ext}}}[1 - \frac{n}{N_{\text{ext}}}]_+$, where $\tau_{\text{ext}} = 48$ h and $N_{\text{ext}} = 10$. Acute attacks can initiate wave-like expanding lesions for highly reactive tissues. For a narrow focal range ($c = 0.25$), damage spreads in a domino-like manner from neuron to neuron. It is contained if glial reaction to cell-death is protective ($D = -1$), but spreads slowly if glial reaction to cell death is inflammatory ($D = 1$). For a wide focal range ($c = 0.75$), a large enough part of the neuronal population needs to be sufficiently damaged to activate the toxic feedback loop. In this case, the lesion spreads quickly, leading to partial and complete cell death for protective and inflammatory glial reactions D, respectively.

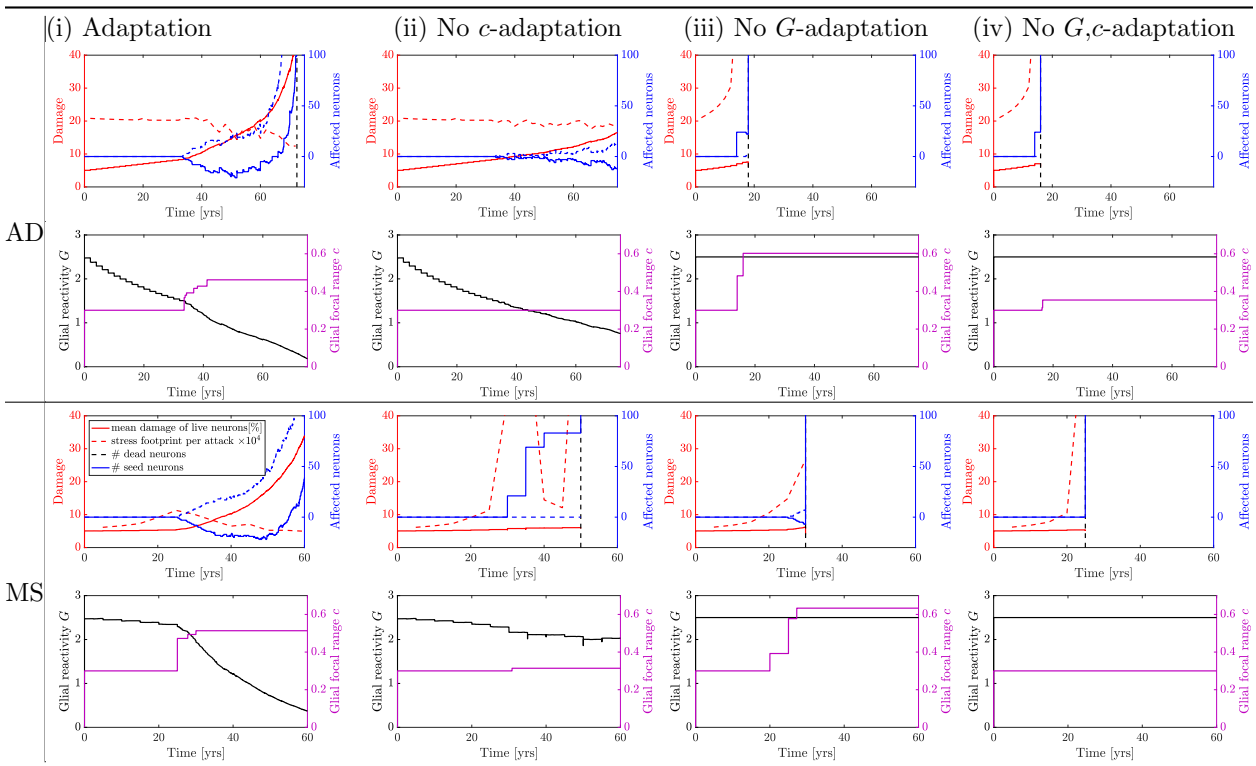

Figure 11: **Lack of adaptation leads to early catastrophic neuron loss:** Effect of adaptation of glial reactivity G and focal range c for an Alzheimer's disease model (AD) and a Multiple Sclerosis disease model (MS). The first column depicts the results as in Fig. 5 of the main manuscript. In the subsequent columns, we deactivate adaptation of c (ii), adaptation of G (iii), and both G and c (iv). In all cases, c is not allowed to adapt beyond 0.6. The black dashed line represents the time point of catastrophic neuron loss of more than 100 neurons (11%). It is seen how no adaptation leads to early catastrophic neuron loss. The AD model is stabilized by G-adaptation, and the MS model is stabilized by both G and c adaptation.